Functional characterization of clinical isolates of the opportunistic fungal pathogen *Aspergillus nidulans*

Rafael Wesley Bastos[a,b,c], Clara Valero[a], Lilian Pereira Silva[a], Taylor Schoen[b,c], Milton Drott[b], Verônica Brauer[d], Rafael Silva-Rocha[d], Abigail Lind[e], Jacob L. Steenwyk[e], Antonis Rokas[e], Fernando Rodrigues[f,g], Agustin Resendiz-Sharpe[h], Katrien Lagrou[h,i], Marina Marcet-Houben[j,k], Toni Gabaldón[j,k,l], Erin McDonnell[m], Ian Reid[m], Adrian Tsang[m], Berl R. Oakley[n], Flávio Vieira Loures[o], Fausto Almeida[d], Anna Huttenlocher[c], Nancy P. Keller[b], Laure Nicolas Annick Ries[d*], and Gustavo H. Goldman[a*]

[a]Faculdade de Ciências Farmacêuticas de Ribeirão Preto, Universidade de São Paulo, Ribeirão Preto, Brazil
[b]Department of Medical Microbiology and Immunology, University of Wisconsin-Madison, Madison, Wisconsin, United States of America
[c]Department of Pediatrics, University of Wisconsin-Madison, Madison, Wisconsin, United States of America
[d]Faculdade de Medicina de Ribeirão Preto, Universidade de São Paulo, Ribeirão Preto, Brazil
[e]Department of Biomedical Informatics, Vanderbilt University School of Medicine, Nashville, Tennessee, United States of America
[f]Life and Health Sciences Research Institute (ICVS), School of Medicine, University of Minho, Braga, Portugal
[7]ICVS/3B's - PT Government Associate Laboratory, Braga/Guimarães, Portugal
[g]Laboratory of Clinical Bacteriology and Mycology, Department of Microbiology, Immunology and Transplantation, KU Leuven, Leuven, Belgium
[h]National Reference Center for Mycosis, University Hospitals Leuven, Leuven, Belgium; Centre for Genomic Regulation (CRG)
[i]Life Sciences Program. Barcelona Supercomputing Centre (BSC-CNS). Jordi Girona, 29. 08034. Barcelona, Spain.
[j]Mechanisms of Disease Program. Institute for Research in Biomedicine (IRB). C/ Baldiri Reixac 10. 08028 Barcelona, Spain.
[l]ICREA, Pg. Lluís Companys 23, 08010 Barcelona, Spain
[m]Centre for Structural and Functional Genomics, Concordia University, Montreal, Quebec, Canada; Department of Molecular Biosciences
[n]University of Kansas , Lawrence , Kansas, United States
[o]Instituto de Ciência e Tecnologia, Universidade Federal de São Paulo, São José dos Campos, Brazil

Running head: Characterization of *Aspergillus nidulans* clinical isolates

#Address correspondence to Gustavo H. Goldman, ggoldman@usp.br; or to Laure NA Ries, rieslaure13@gmail.com

Laure Nicolas Annick Ries and Gustavo Henrique Goldman jointly supervised the work

Abstract

Aspergillus nidulans is an opportunistic fungal pathogen in patients with immunodeficiency and virulence of *A. nidulans* isolates has mainly been studied in the context of the chronic granulomatous disease (CGD), with characterization of clinical isolates obtained from non-CGD patients remaining elusive. This study therefore carried out a detailed biological characterization of two *A. nidulans* clinical isolates (CIs), obtained from a patient with breast carcinoma and pneumonia and from a patient with cystic fibrosis that underwent lung transplantation, and compared them to the reference, non-clinical A4 strain. Both CIs presented increased growth in comparison to the reference strain in the presence of physiologically-relevant carbon sources. Metabolomic analyses showed that the three strains are metabolically very different from each other in these carbon sources. Furthermore, the CIs were highly susceptible to cell wall perturbing agents but not to other physiologically-relevant stresses. Genome analyses identified several frame-shift variants in genes encoding cell wall integrity (CWI) signalling components. Significant differences in CWI signalling were confirmed by western blotting among the three strains. *In vivo* virulence studies using several different models revealed that strain MO80069 had significantly higher virulence in hosts with impaired neutrophil function when compared to the other strains. In summary, this study presents detailed biological characterization of two *A. nidulans sensu stricto* clinical isolates. Just like in *A. fumigatus*, strain heterogeneity exists in *A. nidulans* clinical strains that can define virulence traits. Further studies are required to fully characterize *A. nidulans* strain-specific virulence traits and pathogenicity.

Importance

Immunocompromised patients are susceptible to infections with opportunistic filamentous fungi from the genus *Aspergillus*. Although *A. fumigatus* is the main etiological agent of *Aspergillus spp*.-related infections, other species, such as *A. nidulans* are prevalent in a condition-specific manner. *A. nidulans* is a predominant infective agent in patients suffering from chronic granulomatous disease (CGD). *A. nidulans* isolates have mainly been studied in the context of CGD, although infection with *A. nidulans* also occurs in non-CGD patients. This study carried out a detailed biological characterization of two non-CGD *A. nidulans* clinical isolates and compared it to a reference strain. Phenotypic, metabolomic and genomic analyses highlight fundamental differences in carbon source utilization, stress responses and maintenance of cell wall integrity among the strains. One clinical strain had increased virulence in models with impaired neutrophil function. Just as in *A. fumigatus*, strain heterogeneity exists in *A. nidulans* clinical strains that can define virulence traits.

Introduction

Fungal pathogen-related infections are now estimated to result in a higher number of human deaths as tuberculosis or malaria alone (1-3). The majority of systemic fungal infections are caused by *Candida spp.*, *Pneumocystis* spp., *Cryptococcus spp.* and *Aspergillus spp*. (4,5). Of the hundreds of known *Aspergillus spp*., only a few cause disease in animals, with the most prominent being *A. fumigatus*, *A. flavus, A. nidulans*, *A. niger* and *A. terreus* (6,7).

The primary route of infection of *Aspergillus spp*. is via the inhalation of conidia (asexual spores). In immunocompetent individuals, inhaled conidia are rapidly cleared by pulmonary resident and recruited neutrophils and macrophages, together preventing the onset of infection (8-10). However, disturbances to the immune system may render an individual susceptible to infection by *Aspergillus spp.* (11). The severity of infection largely depends on fungal species and genotype, the host immunological status and host lung structure (6). Invasive Aspergillosis (IA) is the most severe disease caused by *Aspergillus spp*., and is characterized by systemic host invasion, resulting in high mortality rates (30-95%) (2,10,11).

Patient populations with the highest risk of IA are those with prolonged neutropenia from intensive myeloablative chemotherapy and those with genetic disorders resulting in primary immune deficiencies, such as chronic granulomatous disease (CGD) (12,13). CGD is a genetic disorder that affects 1 in 250,000 people and in ~80% of all cases subjects are of the male sex. CGD is caused by mutations in the genes encoding any of the five structural components of the Nicotinamide Adenine Dinucleotide Phosphate (NADPH) –

120 oxidase complex, an enzyme complex important for superoxide anion and
121 downstream reactive oxygen species (ROS) production in phagocytic cells (14).
122 As a result, immune cells are unable to efficiently kill microorganisms and these
123 microorganisms can then become pathogenic in such patients (13,14)

124 Although *A. fumigatus* is the main etiological agent of *Aspergillus*-related
125 infections in immunocompromised patients; other *Aspergillus* spp. have been
126 found to have a high infection rate under some conditions. *A. nidulans* infections
127 are not commonly reported in immunocompromised patients, except for
128 subjects suffering from CGD (15,16). In CGD patients, *A. fumigatus* and *A.*
129 *nidulans* are responsible for 44% and 23% respectively, of all fungal infections
130 (15,16). Infections with *A. nidulans* cause mortality in 27-32% of CGD patients
131 (15) and in comparison to *A. fumigatus*, *A. nidulans* isolates have higher
132 virulence, invasiveness and dissemination, and resistance to antifungal drugs in
133 these patients (17). Hence, *A. nidulans* infections have been studied mainly in
134 the context of CGD although this fungal species can also be virulent in non-
135 CGD, immunocompromised patients (18). In comparison to *A. fumigatus*,
136 investigations into *A. nidulans* isolate virulence have been neglected with very
137 few studies having investigated the genetic and metabolic features of *A.*
138 *nidulans* clinical strains, isolated from CGD and non-CGD patients, in the
139 context of stress responses encountered during human host infection as well as
140 when interacting with host immune responses (18-21).

141 The aim of this work was to carry out a detailed molecular, phenotypic
142 and virulence characterization of two *A. nidulans* clinical isolates from a) a
143 patient with breast carcinoma and pneumonia and b) a patient with cystic

144 fibrosis who underwent lung transplantation and compare them to the well-
145 characterized, wild-type isolate FGSC A4.

146 **Results**

147 **The *A. nidulans* clinical isolates have increased growth, in comparison to**
148 **the reference strain, in the presence of alternative carbon sources**

149 Fungal metabolic plasticity, which allows growth in unique and diverse
150 ambient and host microenvironments, has long been hypothesized to contribute
151 to *Aspergillus* virulence, with carbon sources such as glucose (22), ethanol (23)
152 and acetate (24) being predicted to be actively used during *in vivo* infection. In
153 addition, fatty acids and lipids are also thought to serve as major nutrient
154 sources during mammalian host colonization as is evident by the importance of
155 key glyoxylate cycle enzymes in fungal virulence (25). We therefore
156 characterized growth, by determining fungal dry weight, of the two *A. nidulans*
157 CIs in the presence of minimal medium (MM) supplemented with different
158 physiologically-relevant carbon sources, namely glucose, acetate, ethanol and
159 lipids, and compared it to the FGSC A4 reference strain. A significant reduction
160 in growth was observed for both CIs in the presence of glucose whereas they
161 had significantly increased growth in the presence of the alternative carbon
162 source ethanol, casamino acid and the lipids Tween 20 (a source of lauric,
163 palmitic, and myristic acids) (26), Tween 80 (which contains principally oleate)
164 (26) and olive oil (triacylglycerols and free fatty acids) (27) (Fig. 1). In contrast,
165 no difference in fungal biomass accumulation was observed in the presence of
166 acetate and the lung-resident glycoprotein mucin (Fig. 1). These results suggest
167 that the *A. nidulans* CIs have improved growth relative to the reference strain in

the presence of most of the alternative carbon sources tested here, including different lipids.

Metabolic profiles differ among the *A. nidulans* clinical isolates and reference strain in the presence of different carbon sources

To further investigate nutrient utilization in the *A. nidulans* CIs, the metabolic profiles of strains MO80069 and SP-2605-48 were determined and compared to the reference strain A4. Metabolomics was carried out on cellular extracts from strains grown for 24 h in fructose-rich MM and then transferred for 16 h to MM supplemented with glucose (CIs present reduced growth), ethanol (CIs had increased growth), acetate and mucin (no difference in growth). A total of 40 different metabolites were identified when strains were grown in the presence of glucose and ethanol, whereas 44 different metabolites were identified when strains were grown in the presence of acetate and mucin (Table S1). When comparing metabolite quantities of strain MO80069 to the reference strain, 18 (45%), 22 (55%), 23 (52%) and 24 (55%) metabolite quantities were significantly (p-value < 0.05) different from the quantities in the reference strain when grown in glucose, ethanol, acetate and mucin respectively (Table S1, Table 1). In strain SP-2505-48, 15 (38%), 23 (58%), 30 (68%) and 14 (32%) metabolite quantities, that were normalized by fungal dry weight, were significantly (p-value < 0.05) different from the quantities in the reference strain in the presence of glucose, ethanol, acetate and mucin respectively (Table S1, Table 1). Principal component analysis (PCA) and Hierarchical clustering analysis (HCA) of identified metabolite quantities showed that the CIs clustered apart from the reference strain and from each other in all tested carbon sources

193 (Fig. S1-S2), indicating that they are metabolically different from the reference
194 strain and from each other.

195 When further focusing on metabolites that were significantly different in
196 quantity between the CIs and the reference strain, we observed that in the
197 presence of glucose and ethanol, the majority of identified metabolites were
198 present in significant lower quantities in comparison with the reference strain;
199 whereas both CIs had significant higher metabolite quantities in the presence of
200 acetate in comparison with the reference strain (Fig. 2A-C). Furthermore, when
201 the *A. nidulans* CIs were cultivated in mucin-rich minimal medium, only 9 out of
202 29 significantly different metabolite quantities were identified in both strains
203 whereas the remaining metabolite quantities were strain-specific, suggesting
204 that the metabolic profiles of the two differed drastically the presence of this
205 carbon source (Fig. 2D).

206 When the CIs were grown in a glucose-rich MM, amino acids were found
207 in lower quantities in both CIs when compared to the reference strain. In
208 contrast, pentose phosphate pathway (PPP) intermediates, glycerol, glycerol
209 derivatives and aromatic amino acids were detected in significantly higher
210 quantities in this carbon source (Fig. 2A). In an ethanol-rich MM, significantly
211 lower quantities of various amino acids as well as of the citric acid cycle
212 intermediate citrate were detected in the CIs; whereas increased quantities of
213 several amino acid pathway intermediates, the carbon compounds glycerol,
214 mannitol and trehalose, PPP intermediates and lactate were detected in the CIs
215 when compared to the reference strain in this carbon source (Fig. 2C). In
216 acetate-rich MM, most identified metabolites, notably a variety of amino acids,
217 were present in significantly higher amounts in the CIs when compared to the

reference strain, with the exception of some amino acids, PPP intermediates, spermidine, rhamnose and urea (Fig. 2B). When strains were grown in mucin-rich MM, differences in the quantities of a variety of amino acids were observed, whereas trehalose was present in significantly lower quantities and urea in significantly higher quantities in both CIs when compared to the reference strain (Fig. 2D). In summary, these results suggest significant differences in amino acid biosynthesis and degradation, carbon source storage compounds and degradation among the different *A. nidulans* strains in a condition-dependent manner.

To determine if any metabolic pathways were specifically enriched in the *A. nidulans* CIs in comparison to the reference strain, pathway enrichment analyses was carried out on the metabolome data from glucose-, ethanol-, acetate- and mucin-grown cultures. In all tested carbon sources, with the exception of mucin for isolate SP-2605-48, there was significant enrichment for aminoacyl-tRNA biosynthesis (Table 2). The pathway constituting the metabolism of arginine and proline, was significantly enriched in both clinical isolates when grown in the presence of glucose and ethanol and in isolate SP-2605-48 when incubated in mucin-rich media (Table 2). When acetate was used as the sole carbon and energy source, enrichment of the metabolism of these amino acids was not observed (Table 2). In addition, metabolites identified for strain SP-2605-48 in the presence of mucin and ethanol showed pathway enrichment in nitrogen metabolism (Table 2). In agreement with the aforementioned differences in amino acid quantities, these results suggest that the Cis exhibit differences in nitrogen metabolism in a carbon source-independent manner when compared to the reference strain.

243

244 **The *A. nidulans* clinical isolates are more sensitive to hydrogen peroxide-**
245 **induced oxidative stress and cell wall-perturbing agents when compared**
246 **to the reference strain**

247 Due to the significant metabolic differences observed between the CIs
248 and the reference strain in the presence of physiological-relevant carbon
249 sources, and that primary metabolism (carbon source utilization) has been
250 shown to impact virulence factors in opportunistic pathogenic fungi (28,29), we
251 hypothesized similar differences could be observed in the presence of
252 physiological-relevant stress conditions. One such virulence factor is the fungal
253 cell wall, which is crucial for protection, interaction with and modulation or
254 evasion of the host immune system (30). In addition, cell wall polysaccharide
255 composition is dependent on carbon source primary metabolism (28,29,31).

256 The production of reactive oxygen species (ROS), such as H_2O_2, and
257 subsequent augmentation of cellular oxidative stress is a strategy employed by
258 the mammalian immune system to combat potential invading pathogenic
259 microorganisms (14). The *A. nidulans* reference strain and the two CIs were
260 therefore grown in the presence of hydrogen peroxide (H_2O_2) and the oxidative
261 stress-inducing compound menadione. Both CIs were more sensitive (reduced
262 growth) to high concentrations of H_2O_2 (Fig. S3A), whereas they were resistant
263 to menadione when compared to the reference strain (Fig. S3B). Furthermore,
264 iron sequestration and elevated body temperature are additional physiological
265 stress responses exerted by the host to prevent and/or control infection
266 progression (32). Strains were therefore grown on iron-poor, glucose-rich
267 minimal medium supplemented without (control) or with the iron chelators BPS

and ferrozine (Fig. S3C), as well as in the presence of increasing temperatures (Fig. S3D). Growth of all strains was similar in these conditions, although strain MO80069 grew slightly more in the presence of the iron chelators (Fig. S3C). Lastly, growth of all strains was assessed in the presence of the cell wall perturbing agents caspofungin, congo red (CR) and calcofluor white (CFW). The echinocandin caspofungin is a competitive inhibitor of the cell wall enzyme β-1,3-glucan synthase (33) while CR and CFW bind to glucan or chitin chains respectively (34,35). CR and CFW therefore interfere with the cross-linking of cell wall polysaccharides, resulting in a reduction of cell wall stability. Both clinical isolates were more sensitive to low and medium concentrations of caspofungin when compared to the reference strain, whereas all three strains grew similarly in the highest tested caspofungin concentration (8 µg/ml) (Fig. 3A). Similarly, both clinical strains were more sensitive to lower concentrations of CR whereas no significant difference in growth was observed in the presence of 50 µg/ml CR between all strains (Fig. 3B). In contrast, the CIs had significantly reduced growth in the presence of all tested CFW concentrations when compared to the reference strain (Fig. 3C).

In summary, the aforementioned results suggest strain-specific differences in the response to different physiological stress conditions and infer that the two *A. nidulans* CIs are more sensitive to cell wall-perturbing agents than the reference strain.

292 **The *A. nidulans* clinical isolates do not display increased resistance to**
293 **azoles and amphotericin B**

294 Since both CIs showed increased susceptibility to caspofungin, an
295 echinocandin that is being used as a second line treatment for fungal infections
296 (33), and to other cell wall-perturbing agents, we expanded our analyses to
297 include two additional antifungal drugs classes. Specifically, we followed the
298 "Guidelines for the Diagnosis and Management of Aspergillosis", which, in most
299 of the cases, recommend to treat aspergillosis with azoles and polyene drugs
300 (11), both of which are known to interfere with the biosynthesis or
301 physicochemical properties of fungal membrane sterols (10). Therefore, we
302 determined the minimal inhibitory concentrations (MIC) of the azoles
303 voriconazole, posaconazole and the polyene amphotericin B for all three
304 strains. No differences in the MICs among all strains to these drugs was
305 observed (Table 3).

306

307 **Cleistothecia formation is impaired in the *A. nidulans* SP-2605-48 strain**

308 *A. nidulans* is known for its easily inducible sexual cycle, which serves as
309 a laboratory-based molecular tool for strain construction and studying fungal
310 sexual reproduction (36). To further characterize *A. nidulans* CI biology, we
311 assessed whether *A. nidulans* CIs are able to undergo sexual reproduction, by
312 performing self- and out-crosses for each clinical strain and the reference strain
313 (control) at 30 and 37 °C.

314 Strains were first crossed with themselves (self-crosses) at 30 °C and 37
315 °C, and cleistothecia formation was observed for all strains at both
316 temperatures, except for strain SP-2605-48 at 37 °C (Table 4). Density of

317 cleistothecia (cleistothecia/cm^2) also varied between strains in a temperature-
318 dependent manner, with the clinical isolates forming fewer cleistothecia per cm^2
319 than when compared to the reference strain at 30 °C and 37 °C (Table 4). In
320 addition, no difference in ascospore viability was observed among strains
321 (Table 4).

322 Out-crosses were performed by crossing the *pyrG* (requirement for
323 uridine and uracil) auxotrophic strains MO80069 and SP-2605-48 with the *paba*
324 (requirement for para-aminobenzoic acid)-deficient strain R21XR135 (Table 6).
325 Strain MO80069 produced cleistothecia at both 30 and 37°C whereas strain SP-
326 2605-48 did not produce any cleistothecia in any of the tested conditions.
327 Density of cleistothecia was very low at 30°C (0.25 cleistothecia/cm^2) but
328 increased to the same number than observed for the self-crosses at 37°C with
329 high ascospore viability in all cases (Table 4).

330

331 **Identification of single nucleotide polymorphisms (SNPs) and copy**
332 **number variations (CNVs) in the *A. nidulans* clinical isolate genomes**

333 The aforementioned phenotyping and metabolomics results indicate
334 differences between the strains that affect traits such as nutrient source
335 utilization and resistance to different stresses. These results are in agreement
336 with studies in *A. fumigatus* that have described great strain heterogeneity in
337 traits such as growth, fitness and enzyme secretion between different
338 environmental and clinical isolates (24,37). Indeed, the number of SNPs,
339 obtained during strain pairwise comparison, in the genomes of different *A.*
340 *fumigatus* strains, range between ~13,500 (24) and ~50,000 (38,39). Strain
341 heterogeneity has therefore mainly been investigated in environmental and

clinical isolates of *A. fumigatus*, whereas similar studies have not been carried out for *A. nidulans* isolates. We therefore decided to determine differences at the genomic level by sequencing the genomes of our two *A. nidulans* CIs and comparing them to the FGSC A4 reference genome.

The genomes of MO80069 and SP-2605-48 aligned at 98.3% and 97.4%, respectively, to the genome of the reference strain FGSC A4 with 99.8% nucleotide identity. On the other hand, 1.5% and 1.9% of the A4 assembled genome did not align to the MO800069 and SP-2605-48 genomes respectively, indicating differences among the genomes of all three strains.

A total of 12,956 and 12,399 SNPs with respect to the A4 reference genome were detected in the genomes of MO80069 and SP-2605-48, respectively (Table 5, Table S2). When comparing the genome of SP-260548 to the genome of MO80069, 12,836 SNPs were detected (Table 5, Table S2). Each SNP mutation was classified as either high, moderate or low, according to their impact on the DNA codon frame and amino acid sequence. High impact type mutations encompass frameshift mutations and stop codon gain/loss, whereas missense mutations, resulting in amino acid changes, are considered as moderate impact-type mutations. Low impact-type mutations contain all synonymous mutations and mutations within gene introns and UTRs (untranslated regions). The genome of MO80069 contained 501 high impact mutations, 6,271 missense (moderate impact) and 6,184 synonymous (low impact) mutations in comparison to the reference genome (Table 5, Table S2). In the genome of SP-2605-48, 465 high impact mutations, 5,896 moderate impact mutations and 6,038 low impact mutations were detected in comparison to the reference genome (Table 5, Table S2). When comparing the genomes of

both CIs, 426 high impact mutations, 6,288 missense mutations and 6,122 synonym mutations were detected (Table 5, Table S2). All non-synonymous mutations were distributed throughout the genomes of both CIs and no clear pattern in mutation accumulation could be observed for any of the 8 chromosomes (Fig. 4-5).

In addition, the genomes of both CIs were screened for large-scale (>50 bps) insertions and deletions (indels). In total, 1169 large-scale indels, consisting of anything between 3 bp to 23 kbp in size, were detected on any of the eight chromosomes of the CIs when compared to the reference strain (Supplementary Table 3). Of these, 348 indels were specifically located in the genome of MO80060, 446 indels were found in the genome of SP-2605-48 only, and 375 indels were located in the genomes of both CIs (Table 5, Supplementary Table 3). The majority of these indels were insertions (Table 5). Of the 375 indels found in the genomes of both CIs, 227 (60.5%) indels differed between the two strains, with the remaining 148 indels being identical for both strains (Supplementary Table 3).

The *A. nidulans* clinical isolates are defect in MpkA accumulation in response to cell wall stress

As this work aimed to characterize metabolic utilization of physiologically-relevant carbon and lipid sources in *A. nidulans* CIs, including acetate and fatty acids, we screened genes encoding proteins important for carbohydrate and lipid utilization, cell wall biosynthesis/remodeling and sexual reproduction for the presence of any of the aforementioned moderate and high impact mutations (Table S4). Moderate impact (missense) mutations were detected in three

392 genes (*hxkA*; *swoM*; *pfka*), encoding proteins involved in glycolysis
393 (hexokinase, glucose-6-phosphate isomerase, 6-phosphofructokinase) in both
394 CIs; whereas four and six missense mutations were found in two genes (*idpA*
395 and *mdhA*) encoding the enzymes isocitrate dehydrogenase and malate
396 dehydrogenase of the tricarboxylic acid cycle in the genomes of MO80069 and
397 SP-2605-48, respectively (Table S4). Similarly, several moderate impact
398 mutations were found in genes encoding enzymes required for C2-associated
399 metabolism (acetate, ethanol and fatty acid), including *farA* (transcription factor
400 regulating fatty acid utilization) and *farB* (transcription factor regulating the
401 utilization of short-chain fatty acids) in both CIs, *facA* (acetyl-coA synthase),
402 *acuM* (transcriptional activator required for gluconeogenesis) and *alcM*
403 (required for ethanol utilization) in SP-2605-48 and *echA* (enoyl-coA hydratase)
404 in MO80069 (Table S4). Genes encoding proteins that function in the glyoxylate
405 cycle also contained missense mutations in both CIs (Table S4). Furthermore, a
406 frameshift mutation was detected in both CIs in *acuL*, encoding a mitochondrial
407 carrier involved in the utilization of carbon sources that are metabolized via the
408 Krebs cycle (40) (Table S4). The aforementioned mutations could underlie the
409 observed differences in phenotypic growth in the presence of different carbon
410 and lipid sources.

411 Due to the absence of cleistothecia formation in strain SP-2605-48, we
412 wondered whether this strain contained any mutations in genes encoding
413 proteins required for *A. nidulans* sexual reproduction. We found 11 and 13
414 mutations in 7 and 9 genes related to mating in MO80069 and SP-2605-48
415 genomes, respectively (Table S4). Those mutations include missense and
416 frameshift mutations in genes involved in the perception of light and dark (*ireA*,

417 *ireB*, *cryA*, *veA*, *velB*), mating processes (*cpcA*, *rosA*, *nosA*) and signal
418 transduction (*gprH* and *gprD*) (Table S4). Indeed, *rosA* was absent in both CIs
419 whereas *ireA* was missing from the genome of SP-2605-48. RosA is a
420 transcriptional repressor of sexual development (41) whereas IreA is a
421 transcription factor required for the blue light response, important for
422 developmental processes, including mating.

423 Lastly, as both Cis were sensitive to cell wall perturbing agents, we
424 screened for mutations in genes encoding enzymes involved in cell wall
425 biosynthesis and degradation. Compared to the FGSC A4 reference genome,
426 we found 159 and 90 mutations in 40 and 34 genes involved in cell wall
427 biosynthesis, integrity and signaling in the genomes of MO80069 and SP-2605-
428 48, respectively (Table S4). The majority of these mutations were moderate
429 impact missense mutations in genes that encode components required for 1,3-β
430 and α-glucan, chitin synthesis and degradation, including various types of
431 glucanases, chitinases and chitin synthases (Table S4). However, 17
432 (MO80069) and 9 (SP-2605-48) mutations were high impact level mutations
433 which occurred in genes AN0550 (putative glucan 1,3-beta-glucosidase),
434 AN0509 (putative chitinase), AN0517 (putative chitinase), AN0549 (putative
435 chitinase), AN9042 (putative alpha-1,3-glucanase), AN6324 (putative α-
436 amylase), AN4504 (putative endo-mannanase) and AN0383 (putative endo-
437 mannanase) (Table S4). In addition, small frameshift mutations were detected
438 in three genes encoding the mitogen-activated protein kinase (MAPK) kinase
439 kinase BckA (AN4887), the MAPK MpkA (AN5666) and the transcription factor
440 RlmA (AN2984) (Table S4). In *A. fumigatus*, BckA and MpkA are components of
441 the cell wall integrity (CWI) pathway, which ensures the integrity of the cell wall

and is activated in response to different cell wall stresses including those exerted by cell wall-targeting anti-fungal drugs (42). RlmA was shown to act downstream of MpkA, regulating cell wall biosynthesis-related genes and this transcription factor is also involved in the direct regulation of MpkA (43). Mutation in *rlmA* was observed only in the genome of strain SP-2648-05.

In order to determine whether the observed frameshift mutations had an impact on CWI signaling, we carried out a western blot of phosphorylated MpkA in the presence of NaCl-induced cell wall stress in all three *A. nidulans* strains. Phosphorylated MpkA levels were normalized by total cellular MpkA. Low levels of phosphorylated MpkA were detected in the absence of NaCl in all three strains, but, whereas MpkA protein levels significantly increased upon cell wall stress in the FGSC A4 reference strain, no phosphorylated MpkA could be detected in both CIs (Fig. 6). These results suggest that the observed frameshift mutations in *mpkA* had an effect on MpkA protein levels in the presence of cell wall stress, potentially being (one of) the cause(s) for the observed increased sensitivity to cell wall-perturbing agents.

The *A. nidulans* clinical isolates do not display increased resistance to *in vitro*-mediated killing by different types of macrophages and neutrophils

Due to the observed phenotypic and genotypic differences, we wondered whether the CIs were different in virulence from the reference strain. Virulence was first characterized in a variety of *in vitro* conditions. Macrophages play an essential role in clearing *Aspergillus spp* conidia from the lung (8), whereas neutrophils are predicted to primarily be responsible for eliminating fungal hyphae (39). To determine whether any strain-specific differences exist in

467 macrophage-mediated phagocytosis and killing, the respective assays were
468 carried out for all three strains in the presence of murine wild-type and *gp91*^{phox}
469 knockout (CGD) macrophages. Macrophages from CGD patients are impaired
470 in eliminating conidia from the lung environment, thus rendering the host more
471 susceptible to fungal infections (20). Both types of macrophages phagocytised a
472 significantly higher number of conidia from both *A. nidulans* clinical isolates
473 (~75%) when compared to the reference strain (~ 50%) (Fig. 7A). Indeed,
474 conidia from all three *A. nidulans* strains had increased viability after
475 phagocytosis by *gp91*^{phox} knockout macrophages than when compared to wild-
476 type macrophages, confirming the inability of this type of macrophage to
477 efficiently kill fungal conidia (Fig. 7B). Despite increased phagocytosis of both
478 CIs, no difference in conidial viability was observed for strain MO80069 when
479 compared to the reference strain, whereas wild-type but not CGD macrophages
480 succeeded in killing significantly more SP-2605-48 conidia (Fig. 7B).

481 When challenged with human PMN (polymorphonuclear) cells, fungal
482 survival was reduced approximately 80% for all three *A. nidulans* strains,
483 indicating that the neutrophils were actively killing the hyphal germlings (Fig.
484 7C). No difference in strain survival was observed for the CIs (Fig. 7C). These
485 results suggest that the *A. nidulans* CIs do not have higher survival rates in the
486 presence of macrophages and neutrophils.

487

488

489

490

491 **Virulence of the *A. nidulans* clinical isolates depends on the host immune**
492 **status**

493 We determined the virulence of both *A. nidulans* CIs in animal models
494 with different immune statuses. As it is well known that *A. fumigatus* strain-
495 specific virulence is highly dependent on the type of host immunosuppression
496 and model (24,37, 43), we sought to determine if this would also be the case for
497 *A. nidulans*. The virulence of *A. nidulans* CIs was assessed in both zebrafish
498 and murine models of pulmonary and invasive aspergillosis. Furthermore, the
499 immune system of each animal was manipulated in order to give rise to either
500 immunocompetent, CGD or neutropenic/neutrophilic models. As with patients,
501 CGD models of both mice (19) and zebrafish (21) are very susceptible to *A.*
502 *nidulans* infections. In both immunocompetent- and CGD-type zebrafish and
503 mice, no difference in virulence between the *A. nidulans* clinical isolates and the
504 reference strain was observed (Fig. 8A-D). However, the CI MO80069 was
505 significantly more virulent in neutropenic mice and zebrafish with impaired
506 neutrophil function when compared to the reference strain, whereas no
507 difference in virulence was observed for strain SP-2605-48 (Fig. 8E-F). These
508 results suggest that, like in *A. fumigatus*, *A. nidulans* virulence depends on the
509 strain and the host immune status.

510

511 **Discussion**

512 *Aspergillus nidulans* is a saprophytic fungus that can act as an
513 opportunistic human pathogen in a host immune status- and genetic condition-
514 dependent manner (15,18,44). Infection with *A. nidulans* is prevalent in patients
515 with chronic granulomatous disease (CGD) and isolates have mainly been

516 characterized in the context of this disorder (14,15). Studies on *A. nidulans*
517 virulence have been carried out in CGD models (animal and cell culture) and
518 virulence characteristics have been compared to the primary human
519 opportunistic fungus *A. fumigatus* (20,21,45,46). *A. fumigatus* infection biology
520 and characterization of strains that were isolated from immunocompromised
521 patients with different conditions have received considerable attention in recent
522 years (24,37,47), whereas similar studies into other pathogenic *Aspergillus spp*.
523 have been neglected, although it is becoming apparent that non-*A. fumigatus*
524 species, including cryptic *Aspergillus* species, also contribute to host infection
525 and invasion (7). This work therefore aimed at providing a detailed phenotypic,
526 metabolic, genomic and virulence characterization of two *A. nidulans* clinical
527 isolates (CIs) that were isolated from non-CGD patients.

528 The first CI (MO80069) was isolated from a patient with breast carcinoma
529 and pneumonia, whereas the other CI (SP-2605-48) was obtained from a
530 patient with cystic fibrosis who underwent lung transplantation. Genome
531 sequencing confirmed these strains to be *A. nidulans sensu stricto* and growth
532 of these strains was characterized in the presence of physiological-relevant
533 carbon sources. Fungi require carbon sources in large quantities in order to
534 sustain biosynthetic processes and actively scavenge for them in their
535 environment, including mammalian hosts (24). Available carbon sources vary
536 according to the patient's immune status and disease progression, with, for
537 example, corticosteroid treatment resulting in an increase of fatty and amino
538 acid concentrations and a decrease of glucose levels in mice lungs (22). Growth
539 of the two *A. nidulans* strains in the presence of different carbon sources,
540 differed significantly from the reference strain, with increased biomass

accumulation being observed in the presence of alternative (ethanol, lipids, amino acids) carbon sources and reduced growth in the presence of glucose. The observed phenotypic differences were corroborated by metabolic and genomic data which found a number of missense and high impact mutations in genes encoding enzymes required for alternative carbon source and glucose utilization. These included missense mutations in genes encoding glycolysis- and citric acid cycle-related enzymes as well as five missense mutations in the transcription factor-encoding gene *farA*, which regulates the utilization of short- and long-chain fatty acids. Whether these mutations alone and/or in combination with other identified gene mutations are responsible for the observed growth phenotypes remains to be determined. Nevertheless, it is noteworthy that these mutations are found in both CIs, suggesting that these strains are able to grow well in nutrient-poor environments, such as the lung, when compared the reference strain, which was isolated from the soil environment. Furthermore, whether these mutations are a result of adaptation to the host environment also remains subject to future investigations.

In addition, we also assessed the resistance of these strains to a variety of physiological-relevant stress conditions by growing them in the presence of oxidative- and cell wall stress-inducing compounds, high temperature, iron limitation and anti-fungal drugs. Some minor strain-specific differences were observed in these conditions, but the CIs were not significantly more resistant to these conditions in comparison to the reference strain, including azole- and polyene-type anti-fungal drugs. It is possible that the patient-specific lung environment, biofilm formation and/or interactions with other microorganisms may result in protection from or in the absence of these stresses, thus resulting

566 in strains that do not have increased stress tolerance. In contrast to *Candida*
567 *albicans*, an opportunistic fungal pathogen which was shown to interact with the
568 gram-negative bacterium *Pseudomonas aeruginosa* to promote colonisation of
569 patients with cystic fibrosis in a condition-dependent manner (48), such
570 interactions have not been investigated for *Aspergillus spp*. *Aspergillus* inter-
571 species interactions in lung microbiomes of patients with and without cystic
572 fibrosis therefore remains an intriguing aspect of fungal pathobiology that
573 warrants further characterization.

574 In contrast, both *A. nidulans* clinical strains were significantly more
575 sensitive to the cell wall perturbing agents calcofluor white, congo red and
576 caspofungin (33-35) than the reference strain. These results suggest
577 differences in cell wall composition and/or organization between the clinical
578 isolates and the reference strain. When analyzing the respective genome
579 sequences, we found 159 and 90 mutations in 40 and 34 genes encoding
580 enzymes required for cell wall glucan and chitin biosynthesis and degradation in
581 strains MO80069 and SP-2605-48, respectively, when compared to the FGSC-
582 A4 reference strain. Of particular interest was the identification of high impact
583 mutations in genes *bckA*, *mpkA*, and *rlmA*, which encode components of the
584 CWI signaling pathway. Indeed, Western blotting confirmed the absence of
585 MpkA phosphorylation in the CIs in the presence of cell wall stress. These
586 results suggest that the observed gene mutations cause an altered CWI
587 response, resulting in increased sensitivity to cell wall perturbing agents. The
588 physiological relevance of these findings remains to be determined.

589 *Aspergillus nidulans* is characterized by an easy inducible sexual cycle
590 as well as by undemanding laboratory-based cultivation and genetic

591 manipulation conditions, and has extensively been used as a model organism to
592 study sexual reproduction and developmental processes (49). Nevertheless, it
593 is unknown whether these traits can also be applied to *A. nidulans* clinical
594 strains and this work therefore assessed the ability of the two CIs to form
595 cleistothecia in self- and out-crosses. Strain MO80069 produced cleistothecia
596 and viable ascospores similar to the reference strain in all tested conditions,
597 whereas strain SP-2605-48 only formed cleistothecia and viable ascospores in
598 self-crosses at 30°C and not 37°C. This suggests that a certain degree of
599 heterogeneity exists with regards to sexual reproduction in *A. nidulans* clinical
600 strains, although a bigger sample size and further studies are required in order
601 to confirm this. Temperature has been shown to influence cleistothecia
602 formation in *Aspergillus spp*. with lower temperatures of 30°C resulting in a
603 higher number of formed cleistothecia (50). Furthermore, we cannot exclude the
604 possibility that strains such as SP-2605-48 may require a different condition for
605 sexual reproduction as it is determined by a series of environmental factors that
606 can either activate or repress sexual development (50). This work identified six
607 missense mutations in four genes (*veA*, *cpcA*, *fhbB* and *gprH*) encoding
608 enzymes involved in sexual development and gene *ireA* was absent in the SP-
609 2605-48 genome when compared to strains FGSC-A4 and MO80069. Genes
610 *veA*, *cpcA*, *fhbB and ireA* encode proteins that are involved in the perception of
611 environmental signals (50), favouring the hypothesis that SP-2605-48 may
612 require different/specific conditions for cleistothecia production, although it
613 remains to be determined whether the aforementioned mutations and *ireA* are
614 directly linked to the absence of cleistothecia production in strain SP-2605-48 in
615 the conditions tested here.

Lastly, this work examined the *in vivo* virulence of the *A. nidulans* CIs in different animal models with a variety of immune statuses, as *A. fumigatus* strain-specific virulence is highly dependent on the type of host immunosuppression and model (24,37,51). No difference in virulence was observed in immunocompetent and CGD murine and zebrafish models whereas strain MO80069 was significantly more virulent in a zebrafish with impaired neutrophil function and a neutropenic murine model of invasive aspergillosis than when compared to strains FGSC-A4 and SP-2605-48. These results suggest that neutrophil recruitment and function at the site of infection are important for controlling *A. nidulans* infection in both vertebrates. Furthermore, results are in agreement with studies on *A. fumigatus* which show that virulence is as much a strain-dependent as it is a host-dependent trait (24,37,39,51). Furthermore, the tested phenotypes and genome mutations appear to not correlate with strain virulence, although sample size has to be increased in order to confirm this in future studies. *Aspergillus* infection biology of mammalian hosts is a multi-factorial and –faceted process that not only depends on strain-specific virulence traits (30), but also on the genetic composition of the host and status of the immune system (52). Furthermore, the composition and inter-species interactions of the lung microbiome also influences pathogenicity of a given microorganism, with interactions between different species shown to influence host immune responses (49,53). *A. fumigatus* is the main etiological agent of *Aspergillus*-related diseases and is predominantly present in the lung environment when compared to other infections caused by *Aspergillus spp*. (7). It is therefore possible that other *Aspergillus spp*., such as *A. nidulans*, remain largely undetected in the lung

641 environment, due to the predominant nature and/or inhibitory function of other
642 fungal species, and where they can grow without the necessity to evolve and
643 adapt to extreme stress conditions. The prevalence and virulence of non-*A.*
644 *fumigatus* species therefore remains a highly interesting and somewhat
645 neglected topic that warrants future detailed studies. In summary, this is the first
646 study that presents extensive phenotypic, metabolic, genomic and virulence
647 characterization of two *A. nidulans* clinical isolates. Just as in *A. fumigatus*,
648 strain heterogeneity exists in *A. nidulans* clinical strains that can define
649 virulence traits. Further studies are required to fully characterize *A. nidulans*
650 strain virulence traits and pathogenicity.
651

652 **Materials and Methods**

653 **Ethics statement**

654 The principles that guide our studies are based on the Declaration of
655 Animal Rights ratified by the UNESCO on the 27th January 1978 in its 8th and
656 14th articles. All protocols used in this study were approved by the local ethics
657 committee for animal experiments from Universidade de São Paulo, Campus
658 Ribeirão Preto (permit number 08.1.1277.53.6). All adult and larval zebrafish
659 procedures were in full compliance with NIH guidelines and approved by the
660 University of Wisconsin-Madison Institutional Animal Care and Use Committee
661 (no. M01570 – 0-02-13).
662

663 **Strains, media, and growth conditions**

664 All strains used in this study are listed in Table 6. *A. nidulans* strain
665 FGSC-A4 was used as a reference strain. In addition to culture macroscopic

features and fungal microscopic morphology analysis, whole genome sequencing and phylogenetic analysis confirmed that both clinical isolates are *A. nidulans* (Fig S4). For phylogenetic tree construction, we compared *CaM*, *BenA*, *RPB2* and *ITS* rDNA sequences, identified using blastN implemented in BLAST+ v2.8.1 (54), to sequences from other species in the *Aspergillus* section *Nidulantes* (55), using a maximum-likelihood tree constructed with MEGA v10.1.1 (56). All strains were maintained in 10% glycerol at -80°C.

Strains were grown either in complete medium or minimal medium as described previously (57). Iron-poor MM was devoid of all iron and supplemented with 200 µM of the iron chelators bathophenanthrolinedisulfonic acid (4,7-diphenyl-1,10-phenanthrolinedisulfonic acid [BPS]) and 300 µM of 3-(2-pyridyl)-5,6-bis(4-phenylsulfonic acid)-1,2,4-triazine (ferrozine). All growth was carried out at 37 °C for the indicated amounts of time, except where stated. Reagents were obtained from Sigma-Aldrich (St. Louis, MO) except where stated. Radial growth was determined by inoculating plates with 10^5 spores of each strain and incubation for 5 days before colony diameter was measured. Where required, the oxidative stress-inducing compound menadione or the cell wall perturbing compounds congo red (CR), caspofungin and calcofluor white (CFW) were added in increasing concentrations. All radial growth was expressed as ratios, dividing colony radial diameter (cm) of growth in the stress condition by colony radial diameter in the control (no stress) condition. To determine fungal dry weight, strains were grown from 3 x 10^6 spores in 30 mL liquid MM supplemented with 1% (w/v) of glucose, acetate, mucin or casamino acid or 1% (v/v) of ethanol, Tween 20 and 80 or olive oil for 48 h (glucose) or

690 72h (others) at 37 °C, 150 rpm. All liquid and solid growth experiments were
691 carried out in biological triplicates.

692 Growth in the presence of H_2O_2 was carried out as serial dilutions (10^5 –
693 10^2 spores) in liquid CM in 24-well plates for 48h in the presence of different
694 concentrations of H_2O_2.

695

696 **Metabolite analysis**

697 Metabolome analysis was performed as described previously (58).
698 Briefly, metabolites were extracted from 5 mg of dry-frozen, mycelial powder of
699 four biological replicates. The polar phase was dried and the derivatized sample
700 was analyzed on a Combi-PAL autosampler (Agilent Technologies GmbH,
701 Waldbronn, Germany) coupled to an Agilent 7890 gas chromatograph coupled
702 to a Leco Pegasus 2 time-of-flight mass spectrometer (LECO, St. Joseph, MI,
703 USA). Chromatograms were exported from the Leco ChromaTOF software v.
704 3.25 to the R software (www.r-project.org). The Target Search R-package was
705 used for peak detection, retention time alignment, and library matching.

706 Metabolites were quantified by the peak intensity of a selective mass and
707 normalized by dividing them by the respective sample dry-weight. Principal
708 component analysis was performed using the pcaMethods bioconductor
709 package (59,60). Pathway enrichment analysis was carried out using
710 MetaboAnalyst (http://www.metaboanalyst.ca/MetaboAnalyst/faces/home.xhtml)
711 (61).

712

713

714

715 **Determination of minimal inhibitory concentrations (MICs)**

716 MICs of amphotericin B, voriconazole and posaconazole, were
717 determined by growing 10^4 spores/well in 96-well plates containing 200 µl/well
718 of RPMI and increasing concentrations of the aforementioned compounds,
719 according to the M38 3rd edition protocol elaborated by the Clinical and
720 Laboratory Standards Institute (62).

721

722 **Induction of cleistothecia formation**

723 Cleistothecia formation through self-crossing was induced by growing the
724 strains on glucose minimal medium (GMM) plates that were sealed airtight and
725 incubated for 14 days at 30 or 37°C. Plates were scanned for the presence of
726 cleistothecia under a light microscope. To assess ascospore viability, five
727 cleistothecia of each strain were collected, cleaned on 4% w/v agar plates and
728 re-suspended in 100 µl water. Ascospores were counted and 100 ascospores
729 were plated on GMM before colony-forming units (CFU) were determined.
730 Cleistothecia density was determined through counting the number of
731 cleistothecia of a certain area and dividing them by the cm^2 of the area.

732 Cleistothecia formation through out-crossing was carried out as
733 described previously (57). To induce *pyrG*$^-$ auxotrophy in strains MO80069 and
734 SP-2605-48 (Table 1), they were grown on GMM plates supplemented with 1.2
735 g/L uridine and uracil (UU) and 0.75 mg/mL 5-fluoroorotic acid (FOA) in the form
736 of a cross until single colonies appeared. Auxotrophy was confirmed by growing
737 strains on GMM with and without UU before strains were crossed with strain
738 R21XR135 (Table 1).

739

740 **DNA extraction, genome sequence, detection of single nucleotide**
741 **polymorphisms (SNPs), insertions and deletions (Indels).**

742 DNA was extracted as described previously (57). Genomes were
743 sequenced using 150-bp Illumina paired-end sequence reads at the Genomic
744 Services Lab of Hudson Alpha (Huntsville, Alabama, USA). Genomic libraries
745 were constructed with the Illumina TruSeq library kit and sequenced on an
746 Illumina HiSeq 2500 sequencer. Samples were sequenced at greater than 180X
747 coverage or depth. Short-read sequences for these strains are available in the
748 NCBI Sequence Read Archive (SRA) under accession number.

749 The Illumina reads were processed with the BBDuk and Tadpole
750 programs of BBMap release 37.34
751 [https://sourceforge.net/projects/bbmap/files/BBMap_37.34.tar.gz/download] to
752 remove sequencing adapters and phiX, and to correct read errors. The
753 *Aspergillus nidulans* FGSC_A4 genome sequence and gene predictions,
754 version s10-m04-r15, were obtained from the Aspergillus Genome Database
755 [http://aspgd.org/]. The processed DNA reads were mapped to the FGSC_A4
756 genome with minimap2 version 2.17 [https://github.com/lh3/minimap2] and
757 variants from the FGSC_A4 sequence were called with Pilon version 1.23
758 [https://github.com/broadinstitute/pilon]. Short indels and nucleotide
759 polymorphisms were recovered from the Pilon VCF files by filtering with vcffilter
760 [https://github.com/vcflib/vcflib] to retain only calls with read coverage deeper
761 than 7, exactly one alternative allele, and alternative allele fraction at least 0.8.
762 Longer indels and sequence polymorphisms were recovered by searching the
763 VCF files for the SVTYPE keyword. Sequence variations inside predicted genes
764 and their effects on predicted protein sequence were identified with a custom

765 Python script. The mitochondrial genome was obtained from the discarded
766 contigs of MaSuRCA. Due to its circular nature, the mitochondrial genome
767 appeared repeated multiple times in a single contig. Lastal
768 (http://last.cbrc.jp/doc/last.html) was used to extract one single copy of the
769 mitochondrial genome using the reference mitochondrion.
770

771 **Detection of large genome deletions and insertions**

772 Genome assemblies of the two clinical isolates were aligned to the FGSC
773 A4 reference genome with nucmer (Kurtz et al., 2004). The alignments were
774 filtered to keep only one-to-one matches. Strain-specific loci were detected by
775 searching the alignment coordinates table for regions of the A4 genome with no
776 match in the clinical isolate genome. Large insertions were detected by
777 searching the alignment coordinates table for regions of the clinical isolate
778 genomes with no match in the A4 genome.
779

780 **Identification of transposon-like regions in the FGSC-A4 reference**
781 **genome**

782 Transposon-like regions were identified by running Pfam (64) on the six
783 translation frames of the complete genome sequence. Regions containing any
784 of the fourteen domains typically known to be associated with transposable
785 elements (Table S1) were collected. Inverted repeats longer than 50 bp and
786 separated by less than 5000 bp were extracted and marked as potential
787 Miniature Inverted-repeat Transposable elements (MITE). The Pfam and MITE
788 locations were combined to form the transposon track.
789

790 **Figure generation**

791 DNAPlotter (65) was used to display the loci of all non-synonymous
792 SNPs and large deletions identified in the two clinical strains when compared to
793 the reference genome of FGSC A4. In addition, the locations of transposon-like
794 regions in the A4 genome are also highlighted using DNAPlotter.

795

796 **Western blotting**

797 Strains were grown from $1x10^7$ spores at 37 °C, 200 rpm, in 50 ml CM for
798 16 h before being exposed to 0.5 M NaCl for 0, 10 and 30 min. Total cellular
799 proteins were extracted according to Fortwendel and colleagues (2010)(66) and
800 quantified according to Hartree and colleagues (1972) (67).

801 For each sample, 60 µg of total intracellular protein were run on a 12%
802 (w/v) SDS-PAGE gel before they were transferred to a polyvinylidene difluoride
803 (PVDF) membrane (GE Healthcare). Phosphorylated MpkA or total MpkA was
804 probed for by incubating the membrane with a 1:5000 dilution of the anti-
805 phospho-p44/42 MAPK (9101; Cell Signaling Technologies) antibody or with a
806 1:5000 dilution of the p44-42 MAPK (Cell Signaling Technology) antibody
807 overnight at 4 °C with shaking. Subsequently, membranes were washed 3 x
808 with TBS-T (2.423 g/l Tris, 8 g/L NaCl, 1 ml /l Tween 20), incubated with a
809 1:5000 dilution of an anti-rabbit IgG horseradish peroxidase (HRP) antibody #
810 7074 (Cell Signaling Technologies) for 1 h at room temperature. MpkA was
811 detected by chemoluminescence using the Western ECL Prime (GE
812 Healthcare) blot detection kit according to the manufacturer's instructions. Films
813 were submitted to densitometric analysis using the ImageJ software
814 (http://rsbweb.nih.gov/ij/index.html). The amount of phosphorylated MpkA was

815 normalized by total MpkA. The *A. fumigatus* Δ*mpkA* strain was used as a
816 negative control (Table 1) (68).
817
818 **Isolation and differentiation of bone marrow-derived murine macrophages**
819 Bone marrow-derived macrophages (BMDMs) were isolated as
820 described previously (69). Briefly, BMDMs were recovered from femurs of
821 C57BL/6 wild-type and *gp91^{phox} knockout* mice and were incubated in BMDM
822 medium [RPMI medium (Gibco) supplemented with 30% (v/v) L929 growth
823 conditioning media, 20% inactivated fetal bovine serum (FBS) (Gibco), 2 mM
824 glutamine and 100 units/mL of penicillin-streptomycin (Life Technologies)]. After
825 4 days, fresh media was added for an additional 3 days before BMDMs were
826 collected.
827
828
829 ***In vitro* phagocytosis and killing assays**
830 Phagocytosis and killing assays of *A. nidulans* conidia by wild-type and
831 *gp91^{phox} knockout* macrophages were carried out according to Bom et al. (2015)
832 (70) with modifications. 24-well plates containing a 15-mm-diameter coverslip in
833 each well (phagocytosis assay) or without any coverslip (killing assay) and 2 x
834 10^5 macrophages per well were incubated in 1 ml of RPMI-FBS [(RPMI medium
835 (Gibco) supplemented with 10% inactivated fetal bovine serum (FBS) (Gibco), 2
836 mM glutamine and 100 units/mL of penicillin-streptomycin (Life Technologies)]
837 at 37 °C, 5% CO_2 for 24 h. Wells were washed with 1 ml of PBS before the
838 same volume of RPMI-FBS medium supplemented with 1 x 10^6 conidia (1:5
839 macrophage/conidium ratio) was added in the same conditions.

To determine phagocytosis, macrophages were incubated with conidia for 1.5 h before the supernatant was removed and 500 µl of PBS containing 3.7% formaldehyde was added for 15 min at room temperature (RT). Sample coverslips were washed with 1 ml of ultrapure water and incubated for 20 min with 500 µl of 0.1 mg/ml CFW (calcufluor white) to stain for the cell wall of non-phagocytised conidia. Samples were washed and coverslips were viewed under a Zeiss Observer Z1 fluorescence microscope. In total, 100 conidia were counted per sample and the phagocytosis index was calculated. Experiments were performed in biological triplicates.

To determine macrophage-induced killing of conidia, macrophages were incubated with conidia for 1.5 h before cell culture supernatants were collected and cytokine concentrations were determined. Macrophages were then washed twice with PBS to remove all non-adherent cells and subsequently lysed with 250 µL of 3% v/v Triton X-100 for 10 min at RT. Serial dilutions of lysed samples were performed in sterile PBS and plated onto CM and incubated at 37 °C for 2 days, before colony forming units (CFU) were determined.

Polymorphonuclear (PMN) cell isolation and spore germination assay

Human PMN cells from fresh venous blood of healthy adult volunteers were isolated according to Drewniak et al. (2013) (71), with modifications. Cells were harvested by centrifugation in isotonic Percoll, lysed, and re-suspended in 4-(2-hydroxyethyl)-1-piperazineethanesulfonic acid-buffered saline solution. *A. nidulans* asexual spores were incubated with PMN cells (1 x 10^5cells/mL; effector: 1:500) in a 96-well plate overnight at 37 ºC in RPMI 1640 medium containing glutamine and 10% fetal calf serum (Life). PMN cells were lysed in a

865 water and a sodium hydroxide (pH 11.0) solution (Sigma-Aldrich) and spore
866 germination was determined using an MTT (thiazolyl blue; Sigma-Aldrich)
867 assay, according to Dos Reis et al., (2011). Strain viability was calculated
868 relative to incubation without PMN cells, which was set at 100% for each
869 sample. The viability of *A. nidulans* germinated spores in the presence of PMN
870 cells, was determined as described previously (32).
871
872 **_In vivo_ immunocompetent, CGD (chronic granulomatous disease) and**
873 **neutrophilic zebrafish infections**

874 We evaluated strain virulence in an established zebrafish-aspergillosis
875 model (72 Wild-type larvae were used as an immunocompetent model. Larvae
876 with a dominant negative Rac2D57N mutation in neutrophils (*mpx:rac2D57N*)
877 (Rosowski et al., 2017) were used as a model of leukocyte adhesion deficiency,
878 where neutrophils do not reach the site of infection, and p22^{phox}-deficient larvae
879 (*p22$^{phox\ (sa11798)}$*) were used as a CGD model (21).
880 Spore preparation and conidium micro-injection into the hindbrain of 2-
881 days post fertilization (dpf) larvae were performed as previously described (72).
882 Briefly, after manual dechorionation of embryos, 3 nL of inoculum or PBS-
883 control were injected into the hindbrain ventricle via the optic vesicle (~50
884 conidia) in anesthetized larvae at approximately 36 h post fertilization.
885
886 **_In vivo_ immunocompetent, CGD (chronic granulomatous disease) and**
887 **neutropenic murine infections**

888 Virulence of the *A. nidulans* strains was determined in
889 immunocompetent, CGD and neutropenic mice. *A. nidulans* conidial
890 suspensions were prepared and viability experiments carried out as described
891 previously (70). Eight to twelve weeks old wild-type (n=10) and *gp91^{phox}*
892 *knockout* (n=7) C57BL/6 male mice were used as immunocompetent and CGD

893 models, respectively. Neutropenia was induced in 7-8 weeks old BALB/c female
894 mice (n=10, weighing between 20 and 22 g) with cyclophosphamide at a
895 concentration of 150 mg per kg, administered intraperitoneally (i.p) on days -4
896 and -1 prior to infection (day 0) and 2 days post-infection. Hydrocortisone
897 acetate (200 mg/kg) was injected subcutaneously on day -3 prior to infection.
898 Mice were anesthetized and submitted to intratracheal (i.t.) infection as
899 previously described (73) with some minor modifications. Briefly, after i.p.
900 injection of ketamine and xylazine, animals were infected with 5.0 x 10^7
901 (immunocompetent) or 1 x 10^6 (CGD) conidia contained in 75 µL of PBS (74) by
902 surgical i.t. (intratracheal) inoculation, which allowed dispensing of the fungal
903 conidia directly into the lungs. Neutropenic mice were infected by intranasal
904 instillation of 1.0 x 10^4 conidia as described previously (70). PBS (phosphate
905 buffered saline) was administered as a negative control for each murine model.
906 Mice were weighed every 24 h from the day of infection and visually
907 inspected twice daily. The endpoint for survival experimentation was identified
908 when a 20% reduction in body weight was recorded, at which time the mice
909 were sacrificed.
910
911 **Statistical analyses**
912 All statistical analyses were performed using GraphPad Prism version
913 7.00 (GraphPad Software, San Diego, CA, USA), with $P < 0.05$ considered
914 significantly different. A two-way analysis of variance (ANOVA) was carried out
915 on all stress response tests; whereas a one-way ANOVA with Tukey post-test
916 was applied for growth in the presence of different carbon sources,
917 phagocytosis index and PMN cell killing assay. Survival curves were plotted by

Kaplan-Meier analysis and results were analyzed using the log rank test. All experiments were repeated at least twice.

Acknowledgements

We would like to thank the Fundação de Amparo à Pesquisa do Estado de São Paulo (FAPESP, São Paulo research foundation), grant numbers 2016/07870-9, 2017/19821-5, LNAR 2017/14159-2, FVL 2018/14762-3 and 2019/00631-7 and the Conselho Nacional de Desenvolvimento Científico e Tecnológico (CNPq) for financial support. JLS and AR were supported by the Howard Hughes Medical Institute through the James H. Gilliam Fellowships for Advanced Study program. FR was supported by the Northern Portugal Regional Operational Programme (NORTE 2020), under the Portugal 2020 Partnership Agreement, through the European Regional Development Fund (FEDER) (NORTE-01-0145-FEDER-000013).

We also thank Dra. Danielle da Glória de Souza (UFMG-Brazil) for helping with *gp91^{phox} knockout* C57BL/6 mice.

The funders had no role in study design, data collection and interpretation, or the decision to submit the work for publication.

References

1. Brown GD, Denning DW, Gow NA, Levitz SM, Netea MG, White, TC. 2012. Hidden killers: human fungal infections. Sci. Transl Med 4,165rv13. 4. https://doi: 10.1126/scitranslmed.3004404.

2. Bongomin F, Smith RM, Park BJ, Jarvis JN, Govender NP, Chiller TM, Denning DW, Loyse A, Boulware DR. 2017. Global and multinational prevalence of fungal diseases-estimate precision. J Fungi 3:57. https:// doi: 10.3390/jof3040057.
3. Almeida F, Rodrigues ML, Coelho C. 2019. The still underestimated problem of fungal diseases worldwide. Front Microbiol 10: 214. https:// doi: 10.3389/fmicb.2019.00214
4. Brown GD, Denning DW, Levitz SM. 2012. Tackling human fungal infections. Science 336, 647. https:// doi: 10.1126/science.1222236.
5. Tufa TB, Denning DW. 2019. The Burden of fungal infections in Ethiopia. J Fungi (Basel) 5(4). pii: E109. https:// doi: 10.3390/jof5040109.
6. Paulussen C, Hallsworth JE, Álvarez-Pérez S, Nierman WC, Hamill PG, Blain D, Rediers H, Lievens B. 2017. Ecology of aspergillosis: insights into the pathogenic potency of *Aspergillus fumigatus* and some other Aspergillus species. Microb Biotechnol 102:296–322. https:// doi: 10.1111/1751-7915.12367.
7. Zakaria A, Osman M, Dabboussi F, Rafei R, Mallat H, Papon N, Bouchara JP, Hamze M. 2020. Recent trends in the epidemiology, diagnosis, treatment, and mechanisms of resistance in clinical *Aspergillus* species: A general review with a special focus on the Middle Eastern and North African region. J Infect Public Health 13:1–10. https:// doi: 10.1016/j.jiph.2019.08.007.
8. Philippe B. Ibrahim-Granet O, Prévost MC, Gougerot-Pocidalo MA, Sanchez Perez M, Van der Meeren A, Latgé JP. 2003. Killing of *Aspergillus fumigatus* by alveolar macrophages is mediated by reactive

967 oxidant intermediates. Infec immun 71:3034–3042. https:// doi:
968 10.1128/IAI.71.6.3034-3042.2003.
969 9. Bonnett CR, Cornish EJ, Harmsen AG, Burritt J.B. 2006. Early neutrophil
970 recruitment and aggregation in the murine lung inhibit germination of
971 *Aspergillus fumigatus* conidia. Infect Immun 74:6528-6539. https://
972 10. Latgé JP, Chamilos G. 2019. *Aspergillus fumigatus* and aspergillosis in
973 2019. Clin Microbiol Rev 33:e00140-18. https:// doi:
974 10.1128/CMR.00140-18.
975 11. Kanj A, Abdallah N, Soubani AO. 2018. The spectrum of pulmonary
976 aspergillosis. Respir Med 141:121–131. https:// doi:
977 10.1016/j.rmed.2018.06.029.
978 12. Segal BH, Leto TL, Gallin JI, Malech HL, Holland SM. 2000. Genetic,
979 biochemical, and clinical features of chronic granulomatous disease.
980 Medicine 79:170–200.
981 13. Segal BH, Holland SM. 2000. Primary phagocytic disorders of childhood.
982 Pediatr Clin North Am 47:1311–1338.
983 14. Ross D. 2016. Chronic granulomatous disease. British Medical Bulletin
984 118:53-66. https:// doi: 10.1093/bmb/ldw009.
985 15. Henriet SS, Verweij PE, Warris A. 2012. *Aspergillus nidulans* and chronic
986 granulomatous disease: a unique host-pathogen interaction. J Infect Dis
987 206:1128–1137. https:// doi: 10.1093/infdis/jis473.
988 16. Henriet SS, Verweij PE, Holland SM, Warris A. 2013. Invasive fungal
989 infections in patients with Chronic Granulomatous Disease. In: Curtis N,
990 Finn A, Pollard A. (eds). Hot Topics in Infection and Immunity in Children

991 IX. Advances in Experimental Medicine and Biology. Springer, New York,
992 NY.
993 17. Segal BH, Romani LR. 2009. Invasive aspergillosis in chronic
994 granulomatous disease. Med Mycol 47 Suppl 1:S282-90. https:// doi:
995 10.1080/13693780902736620.
996 18. Tavakoli M, Rivero-Menendez O, Abastabar M, Hedayati MT, Sabino R,
997 Siopi M, Zarrinfar H, Nouripour-Sisakht S, van der Lee H, Valadan R,
998 Meletiadis J, Yazdani Charati J, Seyedmousavi S, Alastruey-Izquierdo A.
999 Genetic diversity and antifungal susceptibility patterns of *Aspergillus*
1000 *nidulans* complex obtained from clinical and environmental sources.
1001 2020. Mycoses 63:78–88. https:// doi: 10.1111/myc.13019.
1002 19. Chang YC, Segal BH, Holland SM, Miller GF, Kwon-Chung KJ. 1998.
1003 Virulence of catalase-deficient aspergillus nidulans in p47(phox)$^{-/-}$ mice.
1004 Implications for fungal pathogenicity and host defense in chronic
1005 granulomatous disease. J Clin Invest 101:1843–1850.
1006 doi:10.1172/JCI2301.
1007 20. Henriet SS, Hermans PW, Verweij PE, Simonetti E, Holland SM, Sugui
1008 JA, Kwon-Chung KJ, Warris A. 2011. Human leukocytes kill *Aspergillus*
1009 *nidulans* by reactive oxygen species-independent mechanisms. Infect
1010 Immun 79:767–773. https:// doi: 10.1128/IAI.00921-10.
1011 21. Schoen TJ, Rosowski EE, Knox BP, Bennin D, Keller NP, Huttenlocher
1012 A. 2019. Neutrophil phagocyte oxidase activity controls invasive fungal
1013 growth and inflammation in zebrafish. J Cell Sci pii: jcs.236539. https://
1014 doi: 10.1242/jcs.236539.

1015 22. Beattie SR, Mark KMK, Thammahong A, Ries LNA, Dhingra S, Caffrey-
1016 Carr AK, Cheng C, Black CC, Bowyer P, Bromley MJ, Obar JJ, Goldman
1017 GH, Cramer RA. 2017. Filamentous fungal carbon catabolite repression
1018 supports metabolic plasticity and stress responses essential for disease
1019 progression. PLoS Pathog 13(4): e1006340. https:// doi:
1020 10.1371/journal.ppat.1006340.
1021 23. Grahl N, Puttikamonkul S, Macdonald JM, Gamcsik MP, Ngo LY, Hohl
1022 TM, Cramer RA. 2011. *In vivo* Hypoxia and a fungal alcohol
1023 dehydrogenase influence the pathogenesis of invasive pulmonary
1024 aspergillosis. Plos Pathog 7: e1002145. https://
1025 doi:10.1371/journal.ppat.1002145
1026 24. Ries LNA, Steenwyk JL, de Castro PA, de Lima PBA, Almeida F, de
1027 Assis LJ, Manfiolli AO, Takahashi-Nakaguchi A, Kusuya Y, Hagiwara D,
1028 Takahashi H, Wang X, Obar JJ, Rokas A, Goldman GH. 2019. Nutritional
1029 heterogeneity among *Aspergillus fumigatus* strains has consequences
1030 for virulence in a strain- and host-dependent manner. Front Microbiol
1031 10:854. https:// doi: 10.3389/fmicb.2019.00854.
1032 25. Olivas I, Royuela M, Romero B, Monteiro MC, Minguez JM, Laborda F,
1033 De Lucas JR. 2008. Ability to grow on lipids accounts for the fully virulent
1034 phenotype in neutropenic mice of *Aspergillus fumigatus* null mutants in
1035 the key glyoxylate cycle enzymes. Fungal Genet Biol 45:45–60.
1036 26. Hynes MJ, Murray SL, Duncan A, Khew GS, Davis MA. 2006. Regulatory
1037 genes controlling fatty acid catabolism and peroxisomal functions in the
1038 filamentous fungus *Aspergillus nidulans*. Eukaryot Cell 5:794–805.

27. Boskou D. 1996. Olive oil composition. Boskou, D. eds. Olive Oil: Chemistry and Technology 1996:52–83 AOCS Press Champaign, IL.

28. Clavaud C, Beauvais A, Barbin L, Munier-Lehmann H, Latgé J-P.n2012. The composition of the culture medium influences the β-1,3-glucan metabolism of *Aspergillus fumigatus* and the anjpegungal activity of inhibitors of β-1,3-glucan synthesis. Antimicrob Agents Chemother 56:3428–3431. https:// doi: 10.1128/AAC.05661-11.

29. Ene IV, Cheng SC, Netea, MG, Brown AJ. 2013. Growth of *Candida albicans* cells on the physiologically relevant carbon source lactate affects their recognition and phagocytosis by immune cells. Infect Immun 81:238–248. https:// doi: 10.1128/IAI.01092-12

30. Abad A, Fernández-Molina JV, Bikandi J, Ramírez A, Margareto J, Sendino J, Hernando FL, Pontón J, Garaizar J, Rementeria A. 2010. What makes *Aspergillus fumigatus* a successful pathogen? Genes and molecules involved in invasive aspergillosis. Rev Iberoam Micol 27:155–182. https:// doi: 10.1016/j.riam.2010.10.003. https://

31. De Assis LJ, Ulas M, Ries LNA, El Ramli NAM, Sarikaya-Bayram O, Braus GH, Bayram O, Goldman GH. 2018. Regulation of *Aspergillus nidulans* CreA-mediated catabolite repression by the F-box proteins Fbx23 and Fbx47. mBio 9:e00840-18. https:// doi: 10.1128/mBio.00840-18. https:// doi: 10.1128/mBio.00840-18.

32. Gazendam RP, van Hamme JL, Tool AT, Hoogenboezem M, van den Berg JM, Prins JM, Vitkov L, van de Veerdonk FL, van den Berg TK, Roos D, Kuijpers TW. 2016. Human neutrophils use different mechanisms to kill *Aspergillus fumigatus* conidia and hyphae: evidence

1064 from phagocyte defects. J Immunol 196:1272–1283. https:// doi:
1065 10.4049/jimmunol.1501811.
1066 33. Aruanno M, Glampedakis E, Lamoth F. 2019. Echinocandins for the
1067 treatment of invasive aspergillosis: from laboratory to bedside.
1068 Antimicrob Agents Chemother 63(8). pii: e00399-19. https:// doi:
1069 10.1128/AAC.00399-19.
1070 34. Kopecka M, Gabriel M. 1992. The influence of congo red on the cell wall
1071 and (1----3)-beta-D-glucan microfibril biogenesis in *Saccharomyces*
1072 *cerevisiae*. Arch Microbiol 158:115–126.
1073 35. Roncero C, Duran A. 1985. Effect of Calcofluor white and Congo redon
1074 fungal wall morphogenesis: in vivo activation of chitin polymerization. J.
1075 Bacteriol 163:1180–1185.
1076 36. Pontecorvo G, Rope, JA, Hemmons LM, Macdonald KD, Bufton AW.
1077 1953. The genetics of *Aspergillus nidulans*. Adv Genet 5:141–238.
1078 37. Kowalski CH, Beattie SR, Fuller KK, McGurk EA, Tang YW, Hohl TM,
1079 Obar JJ, Cramer RA Jr. 2016. Heterogeneity among isolates reveals that
1080 fitness in low oxygen correlates with *Aspergillus fumigatus* virulence.
1081 mBio 7:e01515-16. https:// doi: 10.1128/mBio.01515-16.
1082 38. Knox BP, Blachowicz A, Palmer JM, Romsdahl J, Huttenlocher A, Wang
1083 CC, Keller NP, Venkateswaran K. 2016. Characterization of *Aspergillus*
1084 *fumigatus* isolates from air and surfaces of the international space
1085 station. mSphere 1:e00227-16.
1086 39. Rosowski EE, Raffa N, Knox BP, Golenberg N, Keller NP, Huttenlocher
1087 A. 2017. Macrophages inhibit *Aspergillus fumigatus* germination and

1088 neutrophil-mediated fungal killing. PLoS Pathog 14: e1007229. https://
1089 doi: 10.1371/journal.ppat.1007229.
1090 40. Flipphi M, Oestreicher N, Nicolas V, Guitton A, Velot C. 2014. The
1091 *Aspergillus nidulans acuL* gene encodes a mitochondrial carrier required
1092 for the utilization of carbon sources that are metabolized via the TCA
1093 cycle. Fungal Genet Biol 68:9-22. https:// doi: 10.1016/j.fgb.2014.04.012.
1094 41. Vienken K, Scherer M, Fischer R. 2005. The Zn(II)2Cys6 putative
1095 *Aspergillus nidulans* transcription factor repressor of sexual development
1096 inhibits sexual development under low- carbon conditions and in
1097 submersed culture. Genetics 169: 619–630.
1098 42. Valiante V, Macheleidt J, Föge M and Brakhage AA. 2015. The
1099 *Aspergillus fumigatus* cell wall integrity signaling pathway: drug target,
1100 compensatory pathways, and virulence. Front Microbiol 6:325. https://
1101 doi: 10.3389/fmicb.2015.00325.
1102 43. Rocha MC, Fabri J, de Godoy KF, de Castro PA, Hori JI, da Cunha AF,
1103 Arentshorst M, Ram AFJ, van den Hondel C, Goldman GH, Malavazi I.
1104 2016. *Aspergillus fumigatus* MADS-box transcription factor rlmA is
1105 required for regulation of the cell wall integrity and virulence. G3
1106 (Bethesda)v6:2983–3002. https:// doi: 10.1534/g3.116.031112.
1107 44. Verweij PE, Varga J, Houbraken J, Rijs AJ, Verduynlunel FM, Blijlevens
1108 NM, Shea YR, Holland SM, Warris A, Melchers WJ, Samson RA. 2008.
1109 *Emericella quadrilineata* as cause of invasive aspergillosis. Emerg Infect
1110 Dis 14:566–572. https:// doi: 10.3201/eid1404.071157

45. Dotis J, Roilides E. 2004. Osteomyelitis due to *Aspergillus* spp. in patients with chronic granulomatous disease: comparison of *Aspergillus nidulans* and *Aspergillus fumigatus*. Int J Infect Dis 8:103-110.

46. Henriet SS, van de Sande WW, Lee MJ, Simonetti E, Momany M, Verweij PE, Rijs AJ, Ferwerda G, Sheppard DC, de Jonge MI, Warris A1. 2016. Decreased cell wall galactosaminogalactan in *Aspergillus nidulans* mediates dysregulated inflammation in the chronic granulomatous disease host. J Interferon Cytokine Res. 2016. 488–498. doi: 10.1089/jir.2015.0095.

47. Caffrey-Carr AK, Kowalski CH, Beattie SR, Blaseg NA., Upshaw CR, Thammahong A, Lust HE, Tang YW, Hohl TM, Cramer RA, Obar JJ. 2017. Interleukin 1α is critical for resistance against highly virulent *Aspergillus fumigatus* isolates. Infect Immun 85:e00661-17. https:// doi: 10.1128/IAI.00661-17.

48. Fourie R, Ells R, Swart CW, Sebolai OM, Albertyn J and Pohl CH.2016. *Candida albicans* and *Pseudomonas aeruginosa*. interaction, with focus on the role of eicosanoids. Front Physiol 7:64. https:// doi: 10.3389/fphys.2016.00064.

49. Ojeda-López M, Chen W, Eagle CE, Gutiérrez G, Jia WL, Swilaiman SS, Huang Z, Park HS, Yu JH, Cánovas D, Dyer PS. 2019. Evolution of asexual and sexual reproduction in the aspergilli. Studies in Mycology 91:37–59. https:// doi: 10.1016/j.simyco.2018.10.002

50. Dyer PS, O'Gorman CM. 2012. Sexual development and cryptic sexuality in fungi: insights from *Aspergillus* species. FEMS Microbiol Rev 36:165–192. https://

1136 51. Fuller KK., Cramer RA., Zegans ME, Dunlap JC, Loros JJ. 2016.
1137 *Aspergillus fumigatus* photobiology illuminates the marked heterogeneity
1138 between isolates. mBio 7:e01517-16. https:// doi: 10.1111/j.1574-
1139 6976.2011.00308.x.
1140 52. Kosmidis C, Denning DW. 2015. The clinical spectrum of pulmonary
1141 aspergillosis. Thorax 70:270277. https:// doi: 10.1136/thoraxjnl-2014-
1142 206291.
1143 53. O'Dwyer DN, Dickson RP, Moore BB. 2016. The lung microbiome,
1144 immunity, and the pathogenesis of chronic lung disease. J Immunol
1145 196:4839–4847. https:// 10.4049/jimmunol.1600279.
1146 54. Camacho C, Coulouris G, Avagyan V, Ma N, Papadopoulos J, Bealer K,
1147 Madden TL. 2009. BLAST+: architecture and applications. BMC
1148 bioinformatics 10(1), 421. https:// doi: 10.1186/1471-2105-10-421.
1149 55. Chen AJ, Frisvad JC, Sun BD, Varga J, Kocsubé S, Dijksterhuis J, Kim
1150 DH, Hong SB, Houbraken J, Samson RA. 2016. *Aspergillus* section
1151 Nidulantes (formerly *Emericella*): Polyphasic taxonomy, chemistry and
1152 biology. Stud Mycol 84:1–118. https:// doi: 10.1016/j.simyco.2016.10.001.
1153 56. Kumar S, Stecher G, Li M, Knyaz C,Tamura K. 2018. MEGA X:
1154 Molecular Evolutionary Genetics Analysis across computing platforms.
1155 Mol Bio Evol 35:1547–1549. https:// doi: 10.1093/molbev/msy096.
1156 57. Ries LNA, Beattie SR, Espeso EA, Cramer RA, Goldman GH. 2016.
1157 Diverse regulation of the CreA carbon catabolite repressor in *Aspergillus*
1158 *nidulans*. Genetics 203:335–352. https:// doi:
1159 10.1534/genetics.116.187872.

58. Ries LNA, José de Assis L, Rodrigues FJS, Caldana C, Rocha MC, Malavazi I, Bayram Ö, Goldman GH. 2018. The *Aspergillus nidulans* pyruvate dehydrogenase kinases are essential to integrate carbon source metabolism. G3 (Bethesda) 8:2445–2463. https:// doi: 10.1534/g3.118.200411.
59. Stacklie WH, Redestig H, Scholz M, Walther D, Selbig J. 2007. pcaMethods–a bioconductor package providing PCA methods for incomplete data. Bioinformatics 23:1164–1167.
60. Huege JL, Krall MC, Steinhauser P, Giavalisco R, Rippka. Tandeau de Marsac N, Steinhauser D. 2011. Sample amount alternatives for data adjustment in comparative cyanobacterial metabolomics. Anal Bioanal Chem 399:3503–3517. https:// doi: 10.1007/s00216-011-4678-z.
61. Chong J, Xia J. 2018. MetaboAnalystR: an R package for flexible and reproducible analysis of metabolomics data. Bioinformatics 27 4313–4314. https:// doi: 10.1093/bioinformatics/bty528
62. Clinical and Laboratory Standards Institute. Reference method for broth dilution antifungal susceptibility testing of filamentous fungi: Approved standard M38-A2. CLSI, Wayne, PA, USA, 2017.
63. Kurtz S, Phillippy A, Delcher AL, Smoot M, Shumway M, Antonescu C, Salzberg SL. 2004. Versatile and open software for comparing large genomes. Genome Biology 5:R12.
64. El-Gebali S, Mistry J, Bateman A, Eddy SR, Luciani A, Potter SC, Qureshi M, Richardson LJ, Salazar GA, Smart A, Sonnhammer ELL, Hirsh L, Paladin L Piovesan D, Tosatto SCE, Finn RD. 2019. Nucleic Acids 47(Database issue):D427-D432. https:// doi: 10.1093/nar/gky995.

65. Carver T, Thomson N, Bleasby A, Berriman M, Parkhill J. 2009. Bioinformatics (Oxford, England) 25: 119–120. https:// 10.1093/bioinformatics/btn578.

66. Fortwendel JR, Juvvadi PR, Perfect BZ, Rogg LE, Perfect JR, Steinbach WJ. 2010. Transcriptional regulation of chitin synthases by calcineurin controls paradoxical growth of *Aspergillus fumigatus* in response to caspofungin. Antimicrob Agents Chemother 54:1555–1563. https:// doi: 10.1128/AAC.00854-09.

67. Hartree EF. 1972. Determination of protein: a modification of the Lowry method that gives a linear photometric response. Anal Biochem 48:422–427.

68. Manfiolli AO, Siqueira FS, dos Reis TF, Van Dijck P, Schrevens S, Hoefgen S, Föge M, Straßburger M, de Assis LJ, Heinekamp T, Rocha MC, Janevska S, Brakhage AA, Malavazi I, Goldman GH, Valiante V. 2019. Mitogen activated protein kinase cross-talk interaction modulates the production of melanins in *Aspergillus fumigatus*. mBio 10:e00215-19. https:// doi: 10.1128/mBio.00215-19.

69. Weischenfeldt J, Porse B. 2008. Bone Marrow-Derived Macrophages (BMM): isolation and applications. Cold Spring Harb Protoc pdb.prot5080 pdb.prot5080. https:// doi: 10.1101/pdb.prot5080.

70. Bom VLP, de Castro PA, Winkelströter LK, Marine M, Hori JI, Ramalho LN, dos Reis TF, Goldman MH, Brown NA, Rajendran R, Ramage G, Walker LA, Munro CA, Rocha MC, Malavazi I, Hagiwara D, Goldman GH. 2015. The *Aspergillus fumigatus* sitA phosphatase homologue is

important for adhesion, cell wall integrity, biofilm formation, and virulence. Eukaryot Cell 14:728–744. https:// doi: 10.1128/EC.00008-15.

71. Drewniak A, Gazendam RP, Tool AT, van Houdt M, Jansen MH, van Hamme JL, van Leeuwen EM, Roos D, Scalais E, de Beaufort C, Janssen H, van den Berg TK, Kuijpers TW. 2013. Invasive fungal infection and impaired neutrophil killing in human CARD9 deficiency. Blood 121:2385–2392. https:// doi: 10.1182/blood-2012-08-450551.
72. Knox BP, Deng Q, Rood M, Eickhoff JC, Keller NP, Huttenlocher A. 2014. Distinct innate immune phagocyte responses to *Aspergillus fumigatus* conidia and hyphae in zebrafish larvae. Eukaryot cell 13:1266–1277. https:// doi: 10.1128/EC.00080-14.
73. Cano LE, Singer-Vermes LM, Vaz CAC, Russo M, Calich VLG. 1995. Pulmonary paracoccidioidomycosis in resistant and susceptible mice: relationship among progression of infection, bronchoalveolar cell activation, cellular immune response, and specific isotype patterns. Infect Immun 63:1777–1783.
74. Guerra ES, Lee CK, Specht CA, Yadav B, Huang H, Akalin A, Huh JR, Mueller C, Levitz SM. 2017. Central role of IL-23 and IL-17 producing eosinophils as immunomodulatory effector cells in acute pulmonary aspergillosis and allergic asthma. PLoS Pathog 13:e1006175. https:// doi: 10.1371/journal.ppat.1006175.

Tables.

Table 1. Number and percentage of identified metabolite quantities that were significantly (*p*-value < 0.05) different in the *A. nidulans* clinical isolates in comparison to the reference strain when strains were grown in the presence of glucose, ethanol, acetate and mucin for 16 h.

Carbon Sources	Differentialy Metabolites Produced (%)	
	MO80069 vs FGSC-A4	**SP-2605-48 vs. FGSC-A4**
Glucose	18/40 (45%)	15/40 (38%)
Ethanol	22/40 (55%)	23/40 (58%)
Acetate	23/44 (52%)	30/44 (68%)
Mucin	24/44 (55%)	14/44 (32%)

Table 2. Significant metabolic pathway enrichments

Carbon source	MO80026	SP-2605-48
Glucose	Aminoacyl-tRNA biosynthesis Arginine and proline metabolism	Aminoacyl-tRNA biosynthesis Arginine and proline metabolism
Acetate	Aminoacyl-tRNA biosynthesis Alanine, aspartate and glutamate metabolism Cyanoamino acid metabolism Valine, leucine and isoleucine metabolism Glycine, serine and threonine metabolism	Aminoacyl-tRNA biosynthesis Beta-alanine metabolism
Ethanol	Aminoacyl-tRNA biosynthesis Arginine and proline metabolism	Aminoacyl-tRNA biosynthesis Arginine and proline metabolism Nitrogen metabolism Alanine, aspartate and glutamate metabolism

Table 3. Minimum inhibitory concentrations (MIC) of voriconazole, posaconazole and amphotericin B on the *A. nidulans* clinical isolates MO80069 and SP-2605-48 and the FGSC-A4 reference strain.

Strains	MIC (µg/mL)		
	Voriconazole	**Posaconazole**	**Amphotericin B**
FGSC-A4	0.25	1.0	2.0
MO80026	0.25	1.0	2.0
SP260548	0.25	1.0	2.0

Table 4. Cleistothecia formation and density and ascospore viability resulting from diverse *A. nidulans* self- and out-crosses (A4 = FGSC-A4 reference strain, MO = MO80069, SP = SP-2605-48).

Temperature	Cross	Cleistothecia production	Cleistothecia density (cleistothecia/cm^2)	Ascospores Viability (%)
30 °C	A4 X A4	Yes	15.0 ± 0.81	91.83 ± 3.53
	MO X MO	Yes	7.0 ± 1.35	92.83 ± 3.96
	SP X SP	Yes	0.25 ± 0.25	89.83 ± 3.51
	MO X R21	Yes	1.25 ± 0.25	94.83 ± 3.85
	SP X R21	No	-	-
37 °C	A4 X A4	Yes	9.75 ± 1.43	90.67 ± 3.62
	MO X MO	Yes	5.25 ± 1.31	92.5 ± 2.76
	SP X SP	No	-	-
	MO X R21	Yes	5 ± 0.40	92.5 ± 1.28
	SP X R21	No	-	-

Table 5. Type and total amount of single nucleotide polymorphisms (SNPs) and long insertions and deletions (indels) detected in the genomes of the *A. nidulans* clinical isolates MO80069 and SP-2605-48 when compared to the FGSC-A4 reference genome or in both clinical strains.

Mutation	MO80069 and FGSC A4	SP-2605-48 and FGSC A4	SP-2605-48 and MO80069
Stop codon gain/loss	149	110	170
Frameshift	352	355	256
Missense	6,271	5,896	6,288
Synonymous	6,184	6,038	6,122
Total SNPs	**12,956**	**12,399**	**12,836**
Insertions	234	308	222
Deletion	114	138	207
Total Indels	**348**	**446**	**375**

1349 **Table 6**. Strains used in this study (NA = not applicable).

Strain	Genotype	Source	Reference
FGSC-A4	Glasgow Wild type *(veA+)*	Soil	Pontecorvo et al (1953)
MO80069	Wild type, clinical isolate	Bronchoalveolar lavage of a patient with breast carcinoma and pneumonia (Portugal)	This study
SP-2605-48	Wild type, clinical isolate	Patient with cystic fibrosis who underwent lung transplantation (Belgium)	This study
R21XR135	*pabaA1;yA2*	NA	This study
MO80069*pyrG-*	*pyrG89*	This study	This study
SP-2605-48 *pyrG-*	*pyrG89*	This study	This study
ΔmpkA	*ΔakuB mpkA::ptrA; PTR*	NA	Manfioli et al. (2019)

1350

1351

1352

1353

1354

1355

1356

1357

1358

1359

1360

1361

1362

1363

1364

1365

Figures Captions

Figure 1. The *A. nidulans* clinical isolates exhibit improved growth in the presence of alternative carbon and lipid sources. Strains were grown in liquid MM supplemented with glucose, acetate, ethanol, mucin, tween 20 and 80, olive oil and casamino acids at 37°C for 48 h (glucose) or 72 h (others) before fungal biomass was freeze-dried and weighed. Standard deviations were determined from biological triplicates with ***p*<0.01; ****p*<0.001; *****p*<0.0001 in a one-way ANOVA with Tukey post-test comparing growth of the clinical isolates to the FGSC-A4 reference strain.

Figure 2. The *A. nidulans* clinical isolates are metabolically different from the reference strain in the presence of different carbon sources. Heat maps depicting log-fold changes of identified metabolite quantities, that were significantly (*p*<0.05) different in the *A. nidulans* clinical isolates MO80069 and SP-2605-48 when compared to the FGSC-A4 reference strain (grey squares depict metabolite quantities that were not detected as significantly different in one of the clinical isolates).

Figure 3. The A. nidulans clinical isolates are more sensitive to the cell wall-perturbing agents. Strains were grown from 105 spores on glucose minimal medium supplemented with increasing concentration of (A) caspofungin, (B) congo red and (C) calcofluor white for 5 days at 37°C. Standard deviations represent biological triplicates with **p<0.01; ***p<0.001; ****p<0.0001 in a two-

way ANOVA test, comparing growth of the clinical isolates to the FGSC-A4 reference strain.

Figure 4. Diagram depicting the location of all detected non-synonymous single nucleotide polymorphisms (SNPs) on the 8 chromosomes (chr I – VIII) of the *A. nidulans* clinical isolates SP-2605-48 and MO80069 in comparison to the FGSC-A4 reference genome.

Figure 5. Diagram depicting the location of all detected small deletions on the 8 chromosomes (chr I – VIII) of the *A. nidulans* clinical isolates SP-2605-48 and MO80069 in comparison to the FGSC-A4 reference genome. Also shown are the location of putative transposons in the *A. nidulans* reference genome.

Figure 6. MpkA is not phosphorylated in the *A. nidulans* clinical isolates MO80069 and SP-2605-48 in the presence of NaCl-induced cell wall stress when compared to the FGSC-A4 reference strain. Strains were grown from $1x10^7$ spores in complete medium for 16 h (control, 0 min) at 37°C before 0.5 M NaCl was added for 10 and 30 min. Total cellular protein was extracted and western blotting was carried out probing for phosphorylated MpkA. Signals were normalized by the amount of total MpkA present in the protein extracts and cellular extracts from the Δ*mpkA* strain were used as a negative control.

Figure 7. The *A. nidulans* clinical isolates MO80069 and SP-2605-48 do not present increased survival in the presence of macrophages and neutrophils. (**A**) Percentage of phagocytised conidia by murine wild-type and $gp91^{phox}$ knockout macrophages. Macrophages were incubated for 1.5 h with conidia from the

1415 respective strains before phagocytised conidia were counted. (**B**) Colony
1416 forming units (CFU) as a measure of conidia viability after passage through
1417 wild-type (wt) and *gp91*^{phox} knockout macrophages. Macrophages were
1418 incubated with the respective conidia for 1.5 h before they were lysed and
1419 contents were plated on complete medium. (**C**) Percentage of viable hyphal
1420 germlings after incubation for 16 h with neutrophils from healthy human donors.
1421 Strain viability was calculated relative to incubation without PMN cells, which
1422 was set at 100% for each sample. Standard deviations represent biological
1423 triplicates with *p<0.05 and **p<0.01 when comparing the clinical isolates to
1424 FGSC-A4; #p<0.05 comparing the same strain in the two types of macrophages
1425 in a one-way ANOVA test with Tukey post-test.
1426
1427 **Figure 8**. *A. nidulans* strain-specific virulence depends on the host immune
1428 status. The virulence of the *A. nidulans* clinical isolates MO80069 and SP-
1429 260548 were tested in murine (**A-E**) and zebrafish (**B-F**) models of pulmonary
1430 and invasive aspergillosis. Animals were manipulated in order to give rise to
1431 either immunocompetent (**A-B**), CGD (chronic granulomatous disease) (**C-D**) or
1432 neutropenic (**E**)/neutrophilic (**F**) models. Shown are survival curves for each
1433 immunosuppression and animal model. No difference in virulence was detected
1434 for all strains in both immunocompetent and CGD mice. Strain MO80069 was
1435 significantly more virulent in neutropenic mice and neutrophilic zebrafish.
1436 **p<0.01; ****p<0.0001 when comparing survival curves of the clinical isolates
1437 to the FGSC-A4 reference strain in a two-way ANOVA test with Tukey post-test.
1438
1439

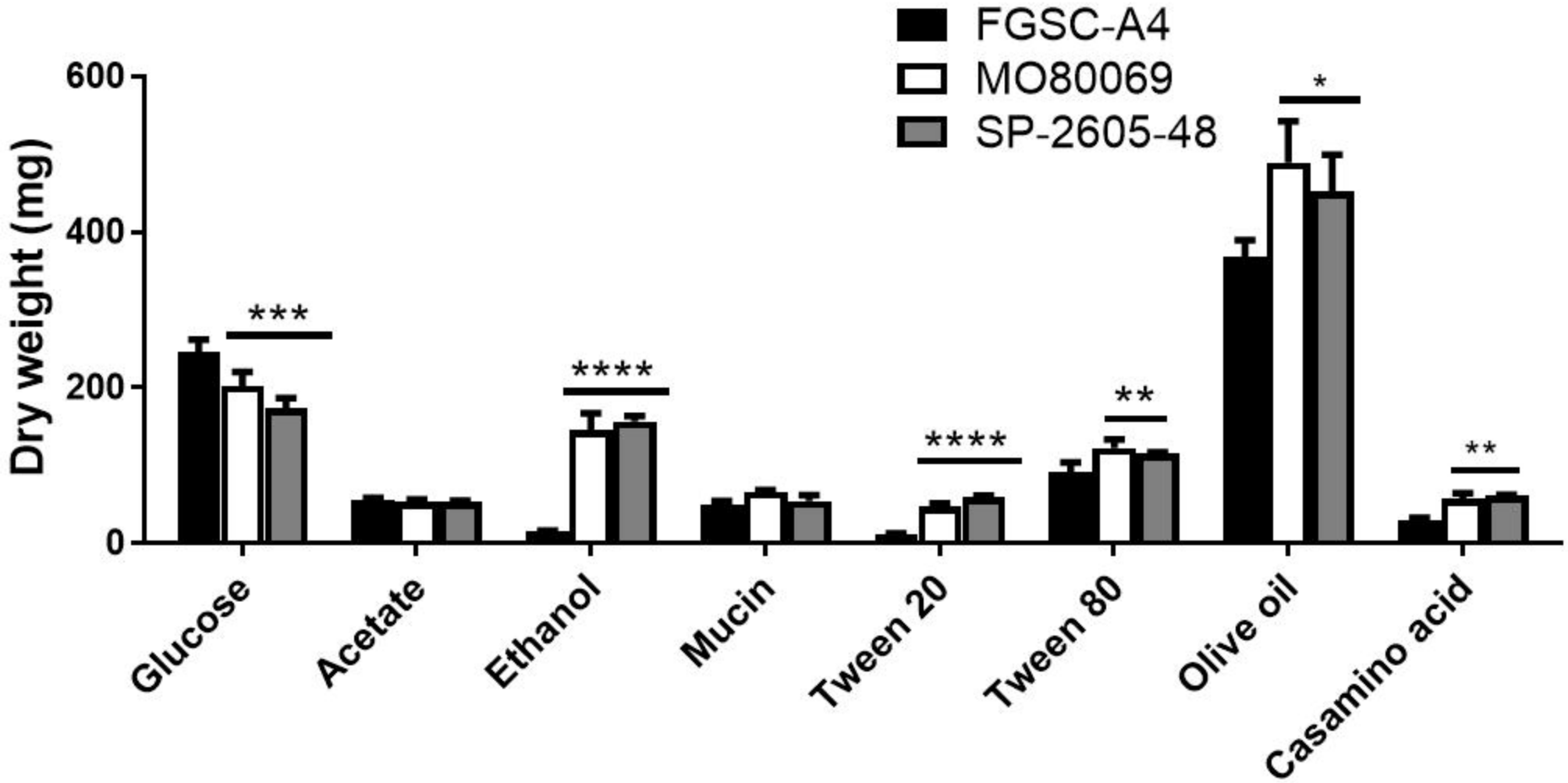
FGSC-A4
MO80069
SP-2605-48
Dry weight (mg)
600
400
200
0
***
****
****
**
*
**
Glucose
Acetate
Ethanol
Mucin
Tween 20
Tween 80
Olive oil
Casamino acid

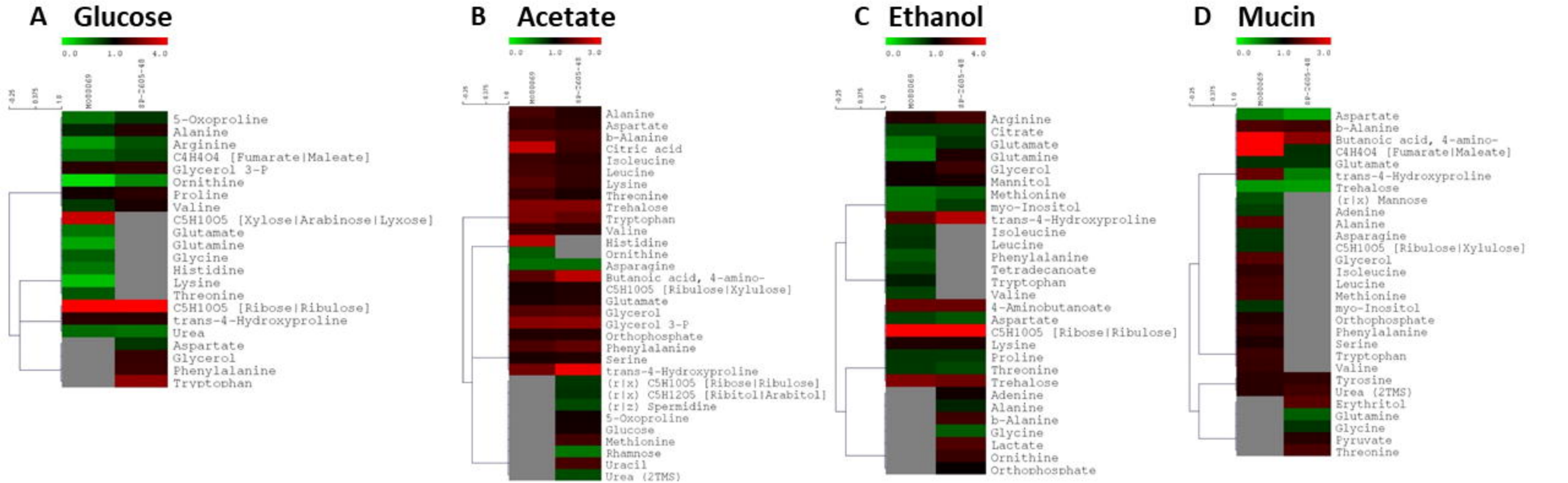
A Glucose
0.0 1.0 4.0
5-Oxoproline
Alanine
Arginine
C4H4O4 [Fumarate|Maleate]
Glycerol 3-P
Ornithine
Proline
Valine
C5H10O5 [Xylose|Arabinose|Lyxose]
Glutamate
Glutamine
Glycine
Histidine
Lysine
Threonine
C5H10O5 [Ribose|Ribulose]
trans-4-Hydroxyproline
Urea
Aspartate
Glycerol
Phenylalanine
Tryptophan
B Acetate
0.0 1.0 3.0
Alanine
Aspartate
b-Alanine
Citric acid
Isoleucine
Leucine
Lysine
Threonine
Trehalose
Tryptophan
Valine
Histidine
Ornithine
Asparagine
Butanoic acid, 4-amino-
C5H10O5 [Ribulose|Xylulose]
Glutamate
Glycerol
Glycerol 3-P
Orthophosphate
Phenylalanine
Serine
trans-4-Hydroxyproline
(r|x) C5H10O5 [Ribose|Ribulose]
(r|x) C5H12O5 [Ribitol|Arabitol]
(r|z) Spermidine
5-Oxoproline
Glucose
Methionine
Rhamnose
Uracil
Urea (2TMS)
C Ethanol
0.0 1.0 4.0
Arginine
Citrate
Glutamate
Glutamine
Glycerol
Mannitol
Methionine
myo-Inositol
trans-4-Hydroxyproline
Isoleucine
Leucine
Phenylalanine
Tetradecanoate
Tryptophan
Valine
4-Aminobutanoate
Aspartate
C5H10O5 [Ribose|Ribulose]
Lysine
Proline
Threonine
Trehalose
Adenine
Alanine
b-Alanine
Glycine
Lactate
Ornithine
Orthophosphate
D Mucin
0.0 1.0 3.0
Aspartate
b-Alanine
Butanoic acid, 4-amino-
C4H4O4 [Fumarate|Maleate]
Glutamate
trans-4-Hydroxyproline
Trehalose
(r|x) Mannose
Adenine
Alanine
Asparagine
C5H10O5 [Ribulose|Xylulose]
Glycerol
Isoleucine
Leucine
Methionine
myo-Inositol
Orthophosphate
Phenylalanine
Serine
Tryptophan
Valine
Tyrosine
Urea (2TMS)
Erythritol
Glutamine
Glycine
Pyruvate
Threonine

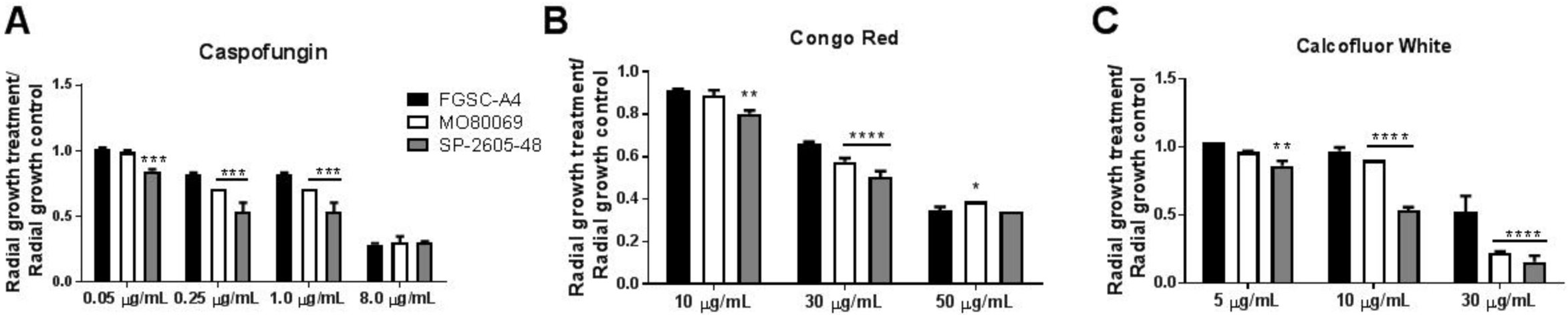
A
Caspofungin
Radial growth treatment/
Radial growth control
1.5
1.0
0.5
0.0
***
***
***
0.05 µg/mL
0.25 µg/mL
1.0 µg/mL
8.0 µg/mL
FGSC-A4
MO80069
SP-2605-48
B
Congo Red
Radial growth treatment/
Radial growth control
1.0
0.8
0.6
0.4
0.2
0.0
**
****
*
10 µg/mL
30 µg/mL
50 µg/mL
C
Calcofluor White
Radial growth treatment/
Radial growth control
1.5
1.0
0.5
0.0
**
****
****
5 µg/mL
10 µg/mL
30 µg/mL

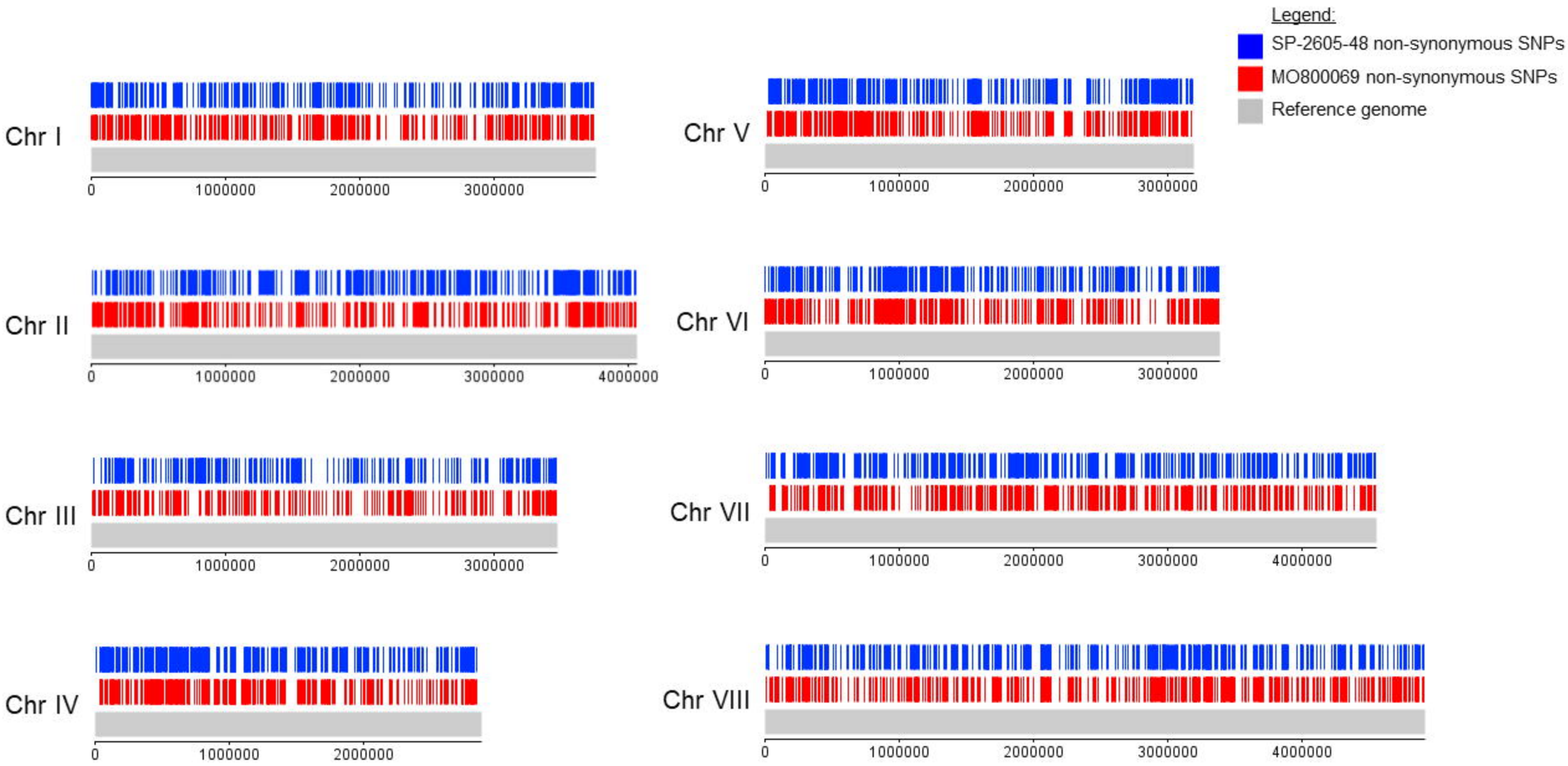
Legend:
SP-2605-48 non-synonymous SNPs
MO800069 non-synonymous SNPs
Reference genome
Chr I
0
1000000
2000000
3000000
Chr II
0
1000000
2000000
3000000
4000000
Chr III
0
1000000
2000000
3000000
Chr IV
0
1000000
2000000
Chr V
0
1000000
2000000
3000000
Chr VI
0
1000000
2000000
3000000
Chr VII
0
1000000
2000000
3000000
4000000
Chr VIII
0
1000000
2000000
3000000
4000000

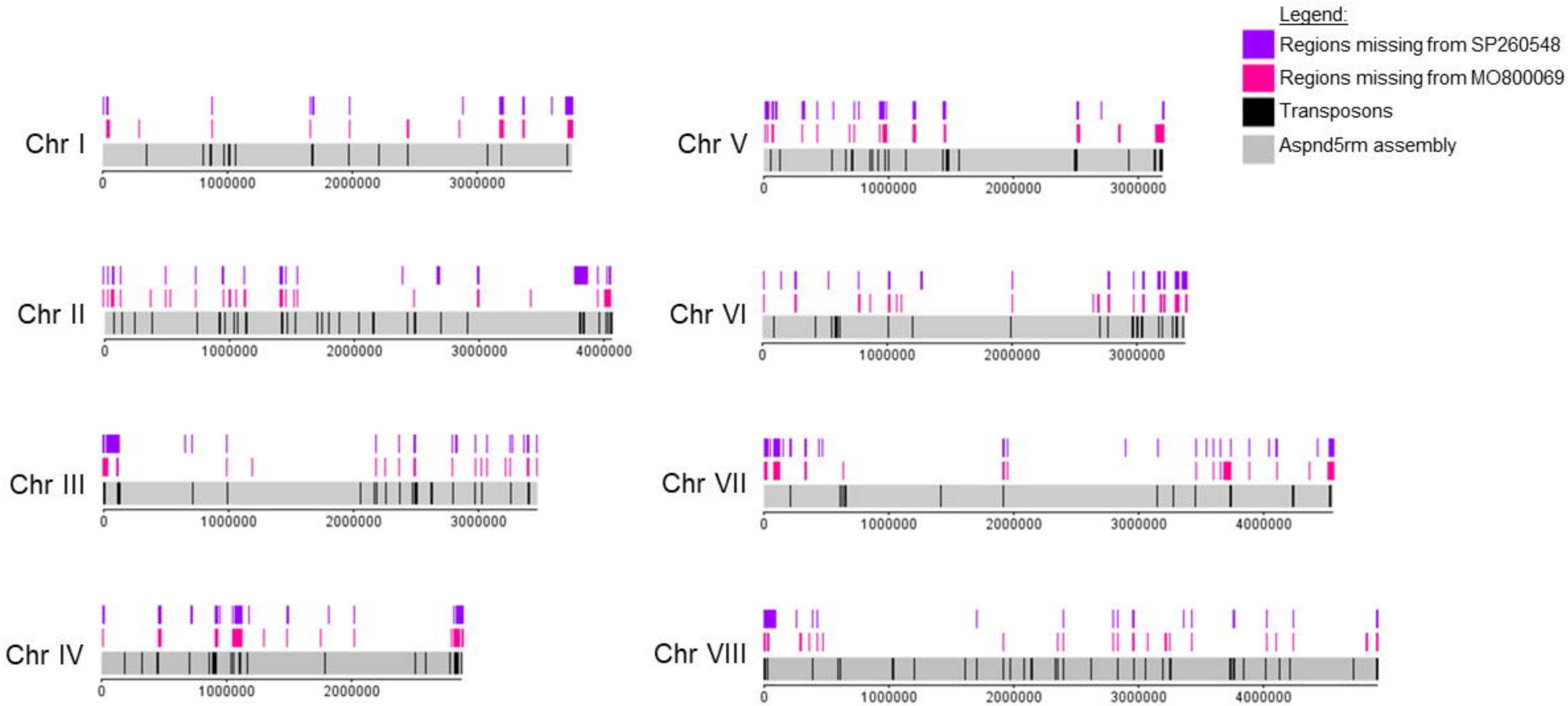
Legend:
Regions missing from SP260548
Regions missing from MO800069
Transposons
Aspnd5rm assembly
Chr I
0
1000000
2000000
3000000
Chr II
0
1000000
2000000
3000000
4000000
Chr III
0
1000000
2000000
3000000
Chr IV
0
1000000
2000000
Chr V
0
1000000
2000000
3000000
Chr VI
0
1000000
2000000
3000000
Chr VII
0
1000000
2000000
3000000
4000000
Chr VIII
0
1000000
2000000
3000000
4000000

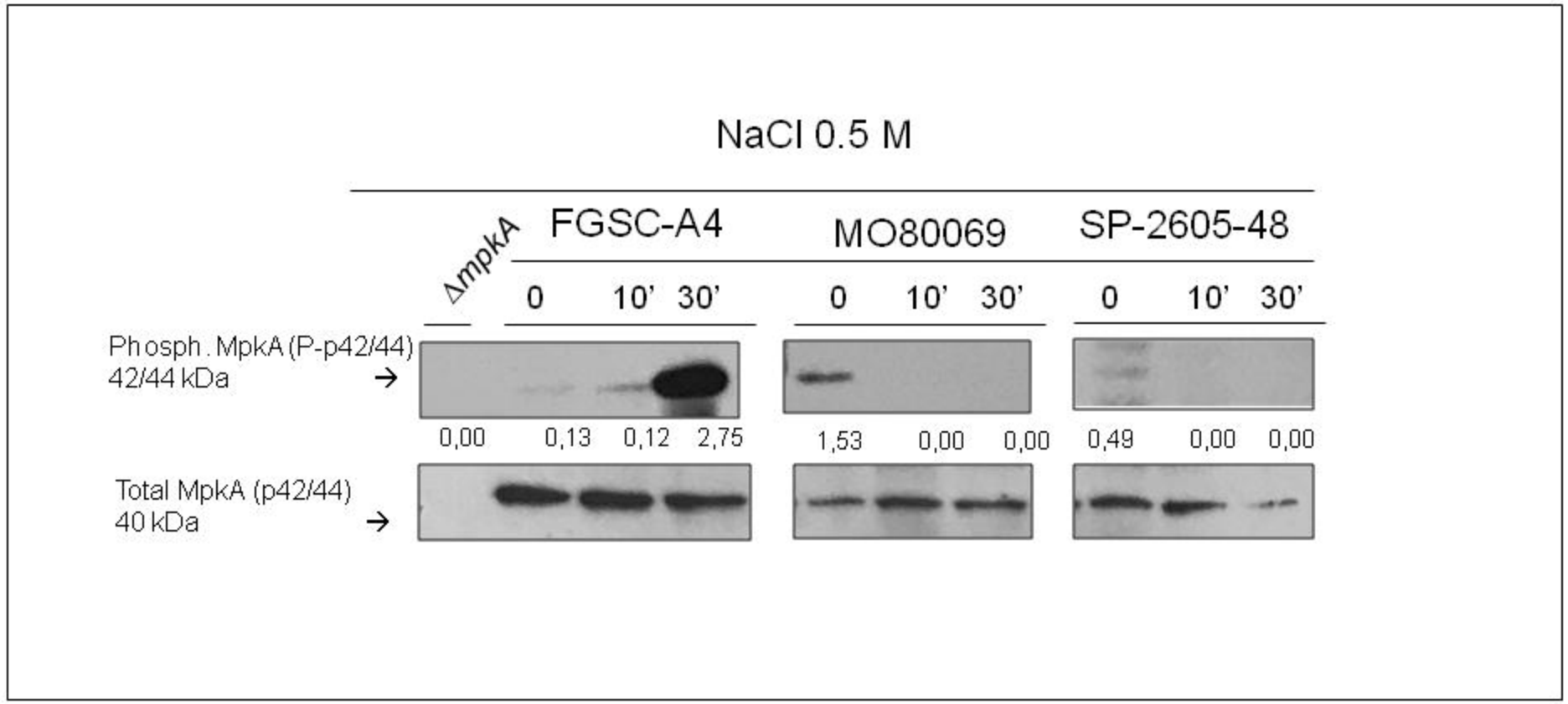
NaCl 0.5 M
ΔmpkA
FGSC-A4
MO80069
SP-2605-48
0
10'
30'
0
10'
30'
0
10'
30'
Phosph. MpkA (P-p42/44)
42/44 kDa
0,00
0,13
0,12
2,75
1,53
0,00
0,00
0,49
0,00
0,00
Total MpkA (p42/44)
40 kDa

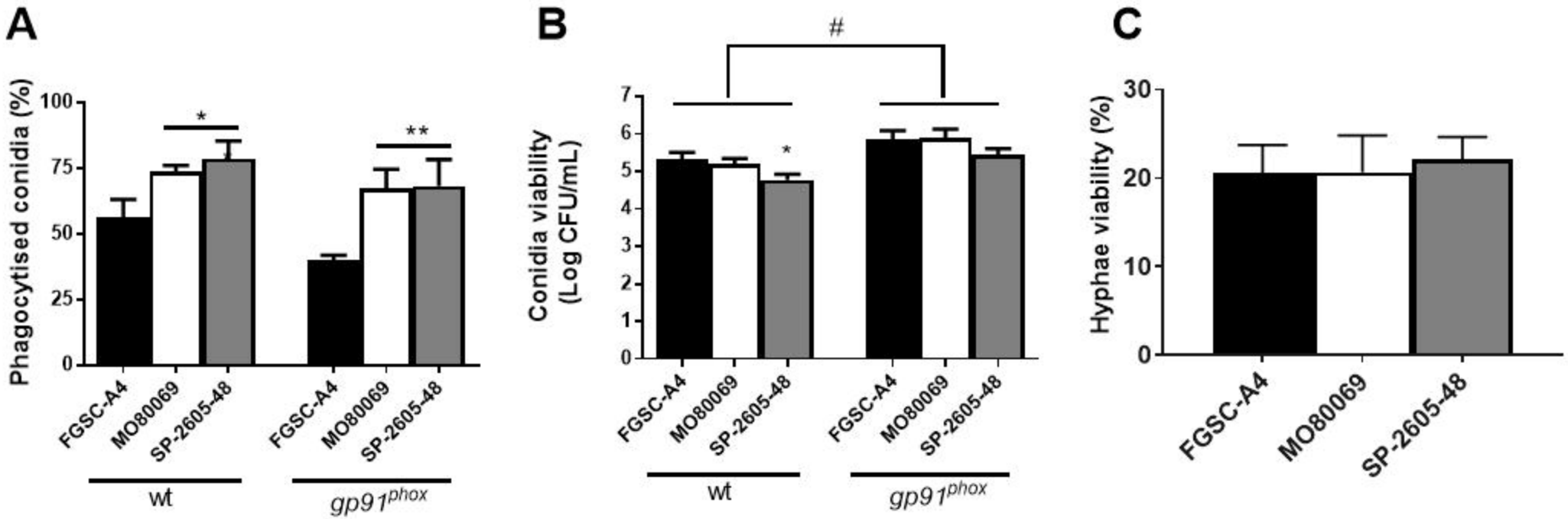
A
Phagocytised conidia (%)
100
75
50
25
0
*
**
FGSC-A4
MO80069
SP-2605-48
FGSC-A4
MO80069
SP-2605-48
wt
gp91phox
B
Conidia viability (Log CFU/mL)
7
6
5
4
3
2
1
0
#
*
FGSC-A4
MO80069
SP-2605-48
FGSC-A4
MO80069
SP-2605-48
wt
gp91phox
C
Hyphae viability (%)
30
20
10
0
FGSC-A4
MO80069
SP-2605-48

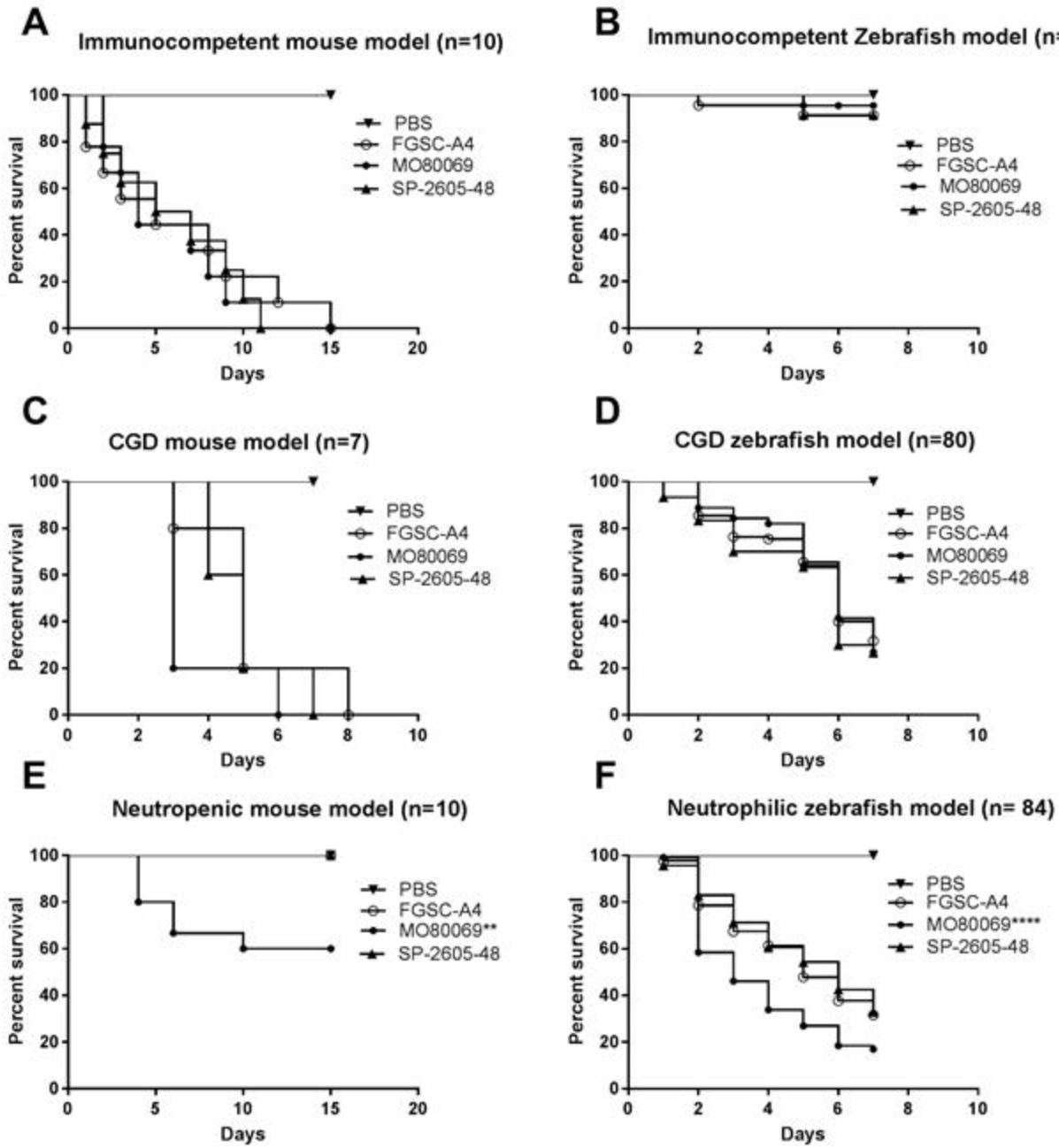
A
Immunocompetent mouse model (n=10)
Percent survival
Days
PBS
FGSC-A4
MO80069
SP-2605-48
B
Immunocompetent Zebrafish model (n=72)
Percent survival
Days
PBS
FGSC-A4
MO80069
SP-2605-48
C
CGD mouse model (n=7)
Percent survival
Days
PBS
FGSC-A4
MO80069
SP-2605-48
D
CGD zebrafish model (n=80)
Percent survival
Days
PBS
FGSC-A4
MO80069
SP-2605-48
E
Neutropenic mouse model (n=10)
Percent survival
Days
PBS
FGSC-A4
MO80069**
SP-2605-48
F
Neutrophilic zebrafish model (n= 84)
Percent survival
Days
PBS
FGSC-A4
MO80069****
SP-2605-48